THE UNIVERSITY OF OKLAHOMA

GRADUATE COLLEGE

A STUDY OF DISTRIBUTED PARAMETERS IN NUCLEAR REACTOR KINETICS

A DISSERTATION

SUBMITTED TO THE GRADUATE FACULTY

in partial fulfillment of the requirements for the

degree of

DOCTOR OF PHILOSOPHY

BY

ALBERT E. UGENE WILSON

Norman, Oklahoma

1964

A STUDY OF DISTRIBUTED PARAMETERS IN NUCLEAR REACTOR KINETICS

APPROVED BY

C. M. Slieppevich

H. W. Rockett

George M. Ewing

Robert M. St. John

Michael L. McGlaun

DISSERTATION COMMITTEE

ACKNOWLEDGMENT

The author wishes to express his sincere gratitude to the many individuals from whom assistance and encouragement have been obtained in the preparation of this dissertation. In particular appreciation is extended to Dr. C. M. Sliepcevich, Research Professor of Engineering, for the advice and stimulation given during his direction of the study.

The assistance and interest of the entire staff of The Nuclear Reactor Laboratory is sincerely appreciated. Reactor Operators, Mr. John V. Boggs and Mr. Johnny James, worked many hours during accumulation of the data. Mr. Harold Cook assisted in the construction of much of the experimental equipment.

Thanks are also extended to The National Science Foundation and The Ford Foundation for financial assistance during the program and to The Atomic Energy Commission for the equipment grants that made the experimental studies possible.

Finally, most sincere thanks are due to my wife, Jeanne, for her encouragement and understanding during the entire graduate program.

TABLE OF CONTENTS

LIST OF TABLES

LIST OF ILLUSTRATIONS

A STUDY OF DISTRIBUTED PARAMETERS IN NUCLEAR REACTOR KINETICS

CHAPTER I

INTRODUCTION

The study of the kinetic behavior of a nuclear reactor is usually based on the nuclear reactor kinetic equations. The equations are:

$$\frac{dn}{dt} = \frac{\Delta k_e - \gamma \beta k_e}{\ell^*} n + \sum_1^6 \gamma_i \lambda_i C_i$$

$$\frac{dC_i}{dt} = \frac{k_e \beta_i}{\ell^*} n - \lambda_i C_i \qquad i = 1 \text{ to } 6$$

$$\sum_1^6 \gamma_i \beta_i = \gamma \beta$$

$$\Delta k_e = k_e - 1$$

where:

n = number of neutrons per cm^3

k_e = effective multiplication factor

ℓ^* = mean neutron lifetime

β = total fraction of neutrons which are delayed

γ = effectiveness of delayed neutrons

C_i = effective concentration of delayed neutron precursors

β_i = fraction of neutrons delayed in i-th group

γ_i = effectiveness of the i-th group of delayed neutrons

λ_i = decay constant of the i-th precursor group

These equations may be developed from the one-energy group, time dependent, diffusion equation for an unreflected homogeneous reactor. A derivation of these equations is given in Appendix A. This particular derivation, which is less rigorous than other derivations found in the literature [1] [2] [3] [4] was developed by the author to point out more clearly the many approximations to the physical system which must be made to arrive at the equations. It is shown that the more important approximations incorporated in these equations are:

1. The medium is homogeneous
2. The medium is a week absorber of neutrons
3. The spatial neutron distribution is the same during transient behavior as at steady state.

The third approximation, which appears to be unrealistic for an

actual reactor, is a result of the assumption that the solution to the time dependent diffusion equation is in the form of a product of a time function and a space function. This assumption is equivalent to stating that the time dependent behavior at any point in space completely describes the time behavior at every other point. For this reason, the kinetic equations given above will be referred to as the "point" model kinetic equations.

The point model kinetic equations may now be linearized and transformed to obtain a conventional transfer function for the reactor. The linearization is accomplished by assuming that k_e, n, and C_i do not deviate far from steady state values so that any terms containing products of the variations may be dropped as negligibly small.

The linearized point model kinetic equations that result from these approximations are shown in Appendix B to be:

$$\frac{d\Delta n}{dt} = \frac{\Delta k_e}{\ell^*} n_0 - \sum_{l=1}^{6} \gamma_i \frac{d\Delta C_i}{dt}$$

$$\frac{d\Delta C_i}{dt} = \frac{\beta_i}{\ell^*} \Delta n - \lambda_i \Delta C_i$$

where

Δn = the variation of the neutron concentration about n_0

ΔC_i = the variation of the i-th precursor concentration about C_{i0}

Since these equations are linear it is possible to obtain a transfer function in terms of the characteristic parameters of the reactor. As shown in Appendix B the reactor gain, G, and the phase shift, θ, may be approximated at frequencies above ten radians per second by:

$$G = 10 \log \frac{1}{1 + \omega^2 T^2}$$

$$\theta = \tan^{-1}(-\omega T)$$

where

ω = frequency in radians per second

T = the smallest system time constant and is given by,

$$T = \frac{\ell^*}{\gamma \beta} .$$

Thus, if the frequency response of the system is measured at frequencies in the neighborhood of $1/T$, the neutron lifetime may be determined from either of the above expressions providing $\gamma\beta$ is known. The values for the β_i have been measured with considerable accuracy by Keepin, Wimett, and Zeigler [27] and the γ_i may be calculated from equations given in Appendix A.

It is apparent that there may be serious errors in the measured values of the system parameters if all of the approximations necessary

to develop the preceding equations are not valid. One case where errors would certainly be possible would be in a very large reactor if the input disturbance were localized in one area. In this case a wave would be propagated through the medium from the point of disturbance. If the response were measured at a point distant from the disturbance one would expect to see at least a time delay relative to a measurement made at a point near the disturbance. The same type of delay would be expected in a small reactor if the effect of the disturbance were measured at a point some distance from the reactor core.

This latter case is of the type encountered in pressurized water or boiling water power reactors. The reactor core is relatively small and, with coolant flow passages, control rods, control rod guides, fuel alignment guides, etc., is quite complex. Little space is available for inserting neutron detection equipment in the core. In addition to the mechanical problem, the core region is at high temperature and the neutron flux is large when the reactor is operated at rated power. Both the temperature and the flux are above the normal operating range of conventional neutron detection equipment. It is the general practice, therefore, to locate the neutron detection equipment outside the core enclosure and base the measurements on the neutron density at the detector rather than on the density in the core. This technique has

limitations even at steady state operation since the effect of control rod shadow, fuel burnup, xenon poisoning, temperature, and other physical changes in core geometry or composition all effect the efficiency of the detector to some extent. These effects cause changes which are relatively slow and calibrations may be made periodically to insure that the detector readings are meaningful.

Dynamic system response of the reactor in the above illustration may be quite different from the response measured at the detector location. The difference in the response is a function of the nuclear properties of the neutron transmission medium between the reactor core and the detector and of the distance separating the two. A lumped parameter model such as the point model kinetic equations cannot account for this difference. It is necessary to include a distributed parameter description of the medium to obtain a model which will include the distance between the reactor core and the detector as a parameter. If such a model is employed, then the response measured at the detector location may be used to calculate the actual reactor response. This model should be as simple as possible but must yield valid results so that it will be useful in experimental measurements in reactor kinetics.

CHAPTER II

REVIEW OF PREVIOUS WORK

An excellent review of early work in the field of nuclear reactor kinetics is presented in Chapter 1.6 of The Reactor Handbook, Volume 1, published by the Atomic Energy Commission in 1955 [1]. This publication is probably the best reference to the classified research sponsored by the Atomic Energy Commission in the early stages of reactor development. Forty of the sixty-four references cited were still classified at the time of publication but the contents were released for reproduction in unclassified documents. The point model kinetic equations are derived and solutions are obtained for various reactivity input functions. No mention is made of the space-time dependence problem which is of primary interest in this paper.

The work cited above has served as a basis for the description of nuclear reactor kinetics in many texts published more recently. Schultz [2] presents essentially the same derivations and solutions with an addition of a graphical method of solution of the non linear equations without linearization. Meghreblian and Holmes [3] perpetuate the same treatment. Weinberg and Wigner [4], although their derivation is more

elegant, end up with the same equations after making the same approximations. Weinberg and Wigner do, however, include a short section on the diffusion of a periodic neutron wave through a moderating medium. Only one energy group is considered so that the relations derived for the propagation velocity of the wave and the attenuation incurred are useful only at large distances from the source where the contribution of fast neutrons is negligible. Also the equations apply only to a good moderator with negligible neutron absorption. Water would certainly not fit the assumptions made in the derivation. Wing [5], in his text on transport theory, includes a rigorous development of the time-dependent; one-dimension, transport problem but the complicated space-time-energy relations that result are not readily applicable to the interpretations of experimental work. His approach is from the mathematicans viewpoint and, as he states in his Preface, "The problems of experimental or theoretical determination of Physical Parameters which arise are ignored altogether."

Most of the work published since 1955 has appeared either in the Journal of the American Nuclear Society, Nuclear Science and Engineering, or in documents issued by Atomic Energy Commission sponsored research groups. The more pertinent articles are presented under the headings of theoretical papers, experimental papers, and related topics in an attempt to organize the material.

Theoretical Papers

An article by A. F. Henry [6] in 1958 is one of the earliest studies of the possible errors involved in assuming space-time separability to develop the nuclear reactor kinetic equations. Henry develops a set of kinetic equations directly from the time dependent transport equation by two different methods. In the first case considered, the property of separability is assumed, the usual approximations are made and the equations previously referred to as the point-model kinetic equations are obtained. In the second case, separability is not assumed and a set of complicated integral equations results. The integrations are performed over all significant variables including the neutron energy, the scattering angle of neutrons suffering elastic scattering and the volume of the system. Since the functions that must be integrated are not usually analytic functions of the variables an iteration procedure is proposed for use with a large digital computer to obtain a solution. The task of treating a physically realistic reactor system by this approach is equivalent to performing the original design calculation many times. Henry gives no experimental work but does suggest experiments in which significant errors might be observed. These suggested experiments involve large changes in reactivity such as reactor shutdown or sudden changes in reflector thickness. He does not present a means of interpreting the proposed experimental work

but suggests tests that may be made to determine the applicability of the point-model kinetic equations to the problem.

Relatively slow changes in the spatial flux distribution considered by Kaplan [7] require a space-time description if the spatial distribution changes are caused by non uniform changes in the parameters of the system. The method proposed involves an approximate solution to the two group time dependent diffusion equations by modal expansion. It is shown that stability problems may be more carefully examined but no experimental work is given. The equations that are developed in this article are applicable to spatial instabilities that result from xenon production or changes in fuel concentration due to burnup. The same type problems are considered by Smets [8] using the point model kinetic equations. Smets obtains the same type of results as those of Kaplan which would indicate that the effect of the separability assumption is not large in relatively slow flux variations.

An extension of the work of Kaplan is reported by Dougherty and Shen [9] in which time dependent coefficients are obtained for a modal expansion of the solution of multigroup kinetic equations. The results, while applicable to a wider range of problems than the results of Kaplan, have the same type of disadvantage mentioned previously for the work of Henry [8]: the indicated integrations are possible only by digital computers since the functions are not analytic. The author

states in his conclusions: "The preceding analysis demonstrates a practical method of solving the space-time neutron kinetic equations for reactor configurations as complicated as the present state of the art allows steady state solutions." No experimental work is reported to support the results.

A modification of the point model kinetic equations to account for neutrons returned to the reactor core from the reflector has been proposed by C. E. Cohn [10]. His modification consists of adding an additional equation to the usual set of equations to account for neutrons which are reflected back to the core region. This modification is equivalent to treating the reflected neutrons as an additional delayed neutron group. The resulting equations after linearization do not differ appreciably from the usual linearized equations except for high frequency variations. It should be noted that the equations developed are applicable in the core region but not in the reflector. Experimental results are included which show qualitatively that the reflected neutrons are important to a description of the core kinetics at frequencies above two hundred cycles per second for the system studied. The importance of this effect will, of course, depend upon the number of neutrons reflected back to the core.

Another approach to the problem of space-time kinetics is presented by Garabedian and Leffert [11] and expanded later by Foderaro

and Garabedian [12]. This method involves expansion of the flux in an infinite series—each term being a product of a space dependent part and a time dependent part. While this approach is not greatly different in principle from the modal expansions cited previously, the resulting equations are somewhat easier to evaluate. Sample calculations are given in the latter article which indicate that the neutron spatial distribution does not remain constant during transient periods and that the separability condition is not satisfied. The time that is predicted for the flux shape to return to that of the steady state is the order of four neutron lifetimes following a rather sizable change in reactivity.

One other problem which has been considered in some detail in the current literature is that of the linearization approximation made to obtain the reactor transfer function from the point model kinetic equations. The problem, however, is not felt to be an important question in the present work. The linearization is necessary only for an interpretation of the experimental results and does not complicate the question of the validity of separability usually assumed.

Experimental Work

A great number of papers have been published describing the experimental methods used in frequency response measurements of nuclear reactors. With few exceptions, these experiments were

performed at low power to obtain the kinetic parameters of the core.

The experiments which employ a sinusoidal variation in reactivity to investigate the frequency response of a nuclear reactor are referred to as reactor oscillator experiments. This type of experiment generally uses a rotating mechanical member to change the reactivity of the system. For thermal reactors the member generally utilizes the high capture cross section of cadmium or boron to effect the reactivity by neutron absorption. Two basic designs have been used for this purpose. The first uses a relatively large diameter rotating member at the edge of the reactor core and relies on the variation of the flux over the diameter and the spatial importance of the neutrons absorbed to change the reactivity. The second uses a rotating segment or segments of a cylindrical cadmium sheet rotating inside fixed cylindrical segments of slightly larger diameter. The surface area of cadmium exposed to the neutron flux is thus a repetitive function. Several such mechanisms are described in the Proceedings of the Conference on Transfer Function Measurement and Reactor Stability Analysis [13].

For fast reactors, rotary reflector rods may be employed. A cylinder with opposite sides cut back will allow greater neutron leakage when flat sides are perpendicular to the side of the reactor than when the flats are parallel to the reactor. This method was used in the frequency analysis of the Los Alamos Molten Plutonium Reactor

experiment [13] [14].

Movable fuel may be used in both thermal and fast reactors but the system complications are increased. Linear, rather than rotary, motion is usually required which greatly increases the power necessary to drive the oscillator if high frequency operation is required.

Recent developments in autocorrelation and crosscorrelation computing equipment have made it possible to perform statistical experiments and extract frequency response data. One of the best reports of experimental work using random reactivity input was by Balcomb, Demuth, and Gyftopoulos [15]. Similar work has been reported by Rajagopal [16] and by Boynton and Uhrig [17]. The work reported by Boynton and Uhrig is of particular interest here since the experiment was performed using a two core reactor with coupling through a graphite region separating the cores. The reactivity change was introduced into one core and the output of the other core was measured. The experimental results indicated that a two point one energy group formulation of the kinetic equations was an adequate description of the system if a constant transit time between the two cores was assumed.

Statistical experiments using reactor noise have also been used

for evaluation of reactor parameters. Less information is obtained but the experiment is considerably simplified since no input reactivity is required. Early work to develop the method was reported by Moore [18] in 1958. This development of the theory led to many experimental studies. One of the most significant by Griffin and Randall [19] compared the results obtained from noise analysis to the results of a reactor oscillator experiment. The results were in general agreement over the frequency range investigated although instrument noise presented more of a problem than had been anticipated.

Related Topics

Neutron Thermalization

Neutron thermalization in moderator materials is fairly well understood and sufficient experimental work has been reported that the group constants necessary for the application of the two group diffusion equations to the diffusion medium may be used with confidence. Some discrepancies still exist--particularly for water--but most of these have been resolved by recent work. The data presented at The Brookhaven Conference on Neutron Thermalization [20] represents the best single source of information in this area. In the introduction to Volume III of these proceedings K. H. Beckurts [21] reviews the previous work and attempts to correlate the work of various authors presenting

papers at the meeting. This survey clearly points out the problems involved in the transport of neutrons in water if the neutrons are not all thermal. The group constants used later in this report have been taken from the Reactor Handbook [1] or from Murray's text [22] with minor corrections as indicated by more recent work.

Neutron Wave Propagation

The study of the propagation of neutron waves through moderating media has been suggested as a means of determining the nuclear properties of the moderator. Perez and Uhrig [23] propose an experiment to evaluate the neutron absorption cross section and the thermal diffusion coefficient in a moderating material by studying the attenuation and phase shift of a wave propagated from a sinusoidally modulated source of neutrons. Their theory is based on a single energy group diffusion equation and is therefore restricted to thermal neutrons. No experimental work is reported in this paper but in an earlier publication by Uhrig [24] the same topic is briefly considered and an indication of the experimental work to support the theory is shown. Very poor agreement between theory and experiment is observed near the neutron source. Since the flux was apparently low in the assembly, the measure- extended only fifteen centimeters from the source and only qualitative agreement was obtained at the larger distances.

Pulse techniques, which are, in a sense, wave propagation studies,

have been used to investigate the nuclear properties of moderating materials, Articles by Garelis and Russel [25] and Garelis [26] consider the problem of using a pulsed source technique to measure neutron lifetime and reactivity in a subcritical facility. The theory is based on a one group diffusion equation and the limited amount of experimental data included in the first paper is in rather poor agreement with the theory.

Reactor Stability

Reactor stability is often the main object in frequency response measurements. In determining the stability of a reactor power plant, the time dependent properties of the reactor must be determined at the operating power of the plant. It is difficult to build and install instrumentation in the core and the reactor parameters are usually determined by instrumentation located some distance from the core. This point is brought out in several papers presented at the conference on Transfer Function Measurement and Reactor Stability Analysis. [13]

CHAPTER III

THEORETICAL CONSIDERATIONS AND STATEMENT OF THE PROBLEM

A model which is useful in the interpretation of experimental data obtained from frequency response testing of a nuclear reactor system in which the reactor core is relatively small but measurements are made at positions outside the core region may be based on the following assumptions:

1. The linearized point model kinetic equations are applicable in the core region of the reactor.
2. Neutron diffusion is a valid mechanism to explain neutron transport through the region outside the core where the measurements are made.
3. The diffusing neutrons may be treated as two energy groups with average group constants applicable to each group.

These assumptions are much less restrictive than the assumptions generally used, and the model developed should be applicable to a large class of testing, research, and power reactors.

Consider first a medium in which diffusion is the principal transport mechanism and in which the diffusing neutrons may be treated as a single energy group. If this medium is outside the core region then no source of neutrons is present and the diffusion equation is

$$D\nabla^2 \phi - \Sigma_a \phi = \frac{1}{v} \frac{\partial \phi}{\partial t} \qquad (1)$$

where

ϕ = neutron flux

D = the diffusion coefficient in the medium

Σ_a = the macroscopic neutron absorption cross section in the medium

v = the average velocity of the neutrons in the energy group considered.

Physical boundary conditions necessary for the solution of equation (1) are that the flux is finite and continuous throughout the medium since no sources are present and that the neutron flux is continuous across the core-diffusion medium interface.

A further simplification will be made for this discussion by assuming that the measurements to be made are all at positions on a major axis and that the system has sufficient symmetry so that neutron variation with respect to the other dimensions is small. Then

$$\frac{\partial \phi}{\partial y} = \frac{\partial \phi}{\partial z} = 0$$

$$D \frac{\partial^2 \phi}{\partial x^2} - \Sigma_a \phi = \frac{1}{v} \frac{\partial \phi}{\partial t}. \qquad (2)$$

If the core region is being driven by a reactivity variation of the form cos ωt then the linearized point kinetic equations would predict that neutron flux variation in the core will be of the same form but will lag by an angle, θ_c, which is frequency dependent. The boundary condition to be applied at the interface between the core and the diffusion medium for equation (2) is therefore:

$$\phi = \phi_0 + \Delta\phi_c \cos(\omega t + \theta_c) \text{ at } x = x_0 \qquad (3)$$

where

x_0 = the position of the interface

ϕ_0 = the average value of the neutron flux at x_0

$\Delta\phi_c$ = the magnitude of the flux variation at x_0.

A function of x and t to describe the neutron flux in the diffusion medium must fit the boundary condition (3) and allow for the finite time of propagation of the variation through the medium. Such a function would be of the form:

$$\phi(x,t) = \phi(x) + \Delta\phi_c \, e^{-b(x-x_0)} \cos[\omega t + \theta_c + a(x-x_0)]. \qquad (4)$$

where

$$\phi(x) = \phi_0 \text{ at } x = x_0.$$

Let

$$\varepsilon(x,t) = \Delta\phi_c \, e^{-b(x-x_0)} \cos\left[\omega t + \theta_c + a(x - x_0)\right]. \tag{5}$$

Then

$$\phi(x,t) = \phi(x) + \varepsilon(x,t).$$

If the above is a solution to equation (2) then

$$D \frac{\partial^2 \phi(x)}{\partial x^2} + D \frac{\partial^2 \varepsilon(x,t)}{\partial x^2} - \Sigma_a \phi(x) - \Sigma_a \varepsilon(x,t) = \frac{1}{v} \frac{\partial \varepsilon(x,t)}{\partial t} \tag{6}$$

but $\phi(x)$ is a function of x only, and the partial derivative may be replaced by the total derivative

$$D \frac{d^2 \phi(x)}{dx^2} - \Sigma_a \phi(x) = 0. \tag{7}$$

Since $\phi(x) = \phi_0$ at $x = x_0$ and the flux is finite for any value of x greater than x_0, the solution to equation (7) is,

$$\phi(x) = \phi_0 \, e^{-\left[\frac{\Sigma_a}{D}\right]^{\frac{1}{2}}(x - x_0)}. \tag{8}$$

Equation (8) is the solution to the one group steady state diffusion equation and indicates that a solution of the form of equation (4) reduces to the accepted solution for steady state conditons.

The remaining portion of equation (6) is,

$$D \frac{\partial^2 \varepsilon(x,t)}{\partial x^2} - \Sigma_a \varepsilon(x,t) = \frac{1}{v} \frac{\partial \varepsilon(x,t)}{\partial t} \tag{9}$$

Substituting equation (5) into equation (9) yields

$$\left(b^2 - a^2 - \frac{\Sigma_a}{D}\right) \cos\left[\omega t + \theta_c + a(x - x_0)\right]$$

$$= \left(\frac{\omega}{vD} + 2ab\right) \sin\left[\omega t + \theta_c + a(x - x_0)\right]. \tag{10}$$

Equation (10) can be true for all values of x and t only if the coefficients of the sine and cosine terms are zero. Therefore:

$$b^2 - a^2 - \frac{\Sigma_a}{D} = 0 \tag{11}$$

$$\frac{\omega}{vD} + 2ab = 0 \tag{12}$$

Equations (11) and (12) may be solved for b^2 and a^2 to obtain

$$b^2 = \frac{\frac{\Sigma_a}{D} + \left[\frac{\Sigma_a^2}{D^2} + \frac{\omega}{v^2 D^2}\right]^{\frac{1}{2}}}{2} \tag{13}$$

$$a^2 = \frac{-\frac{\Sigma_a}{D} + \left[\frac{\Sigma_a^2}{D^2} + \frac{\omega}{v^2 D^2}\right]^{\frac{1}{2}}}{2} \tag{14}$$

Equations (13) and (14) may be simplified by recognizing that for

neutron velocities and oscillator frequencies of practical interest,

$$\frac{\omega^2}{v^2 D^2} \ll \frac{\Sigma_a^2}{D^2} \tag{15}$$

so that

$$\left[\frac{\Sigma_a^2}{D^2} + \frac{\omega^2}{v^2 D^2}\right]^{\frac{1}{2}} \cong \frac{\Sigma_a}{D} + \frac{\omega^2}{2 \Sigma_a D v^2} . \tag{16}$$

The application of the approximation in equation (16) to the expressions for b^2 and a^2 of equations (13) and (14) yields

$$b \cong \left[\frac{\Sigma_a}{D} + \frac{\omega^2}{4 \Sigma_a D v^2}\right]^{\frac{1}{2}} \tag{17}$$

$$a \cong \pm \frac{\omega}{2v} \left[\frac{1}{\Sigma_a D}\right]^{\frac{1}{2}} \tag{18}$$

where the signs of b and a have been chosen to satisfy the boundary conditions previously specified.

Equations (17) and (18) indicate, at least qualitatively, the dependence of phase shift and attenuation on the neutron velocity in the diffusion medium. Since the neutrons being fed into the medium at the core interface have energies ranging from a few

thousandths of an electron volt to several million electron volts, the one energy group formulation presented above cannot be expected to describe the system accurately. The results can be used, however, to predict the form of the solution to be expected when energy is included as a parameter. It will be shown that two energy groups are adequate to describe a system in which the diffusion medium acts as a neutron moderator if the energies of the two groups are properly chosen.

Two-group, one-dimension, time-dependent, neutron diffusion is described by a pair of equations rather than a single equation as in (2). These equations are:

$$D_1 \frac{\partial^2 \phi_1}{\partial x^2} - \Sigma_1 \phi_1 = \frac{1}{v} \frac{\partial \phi_1}{\partial t} \tag{19}$$

$$D_2 \frac{\partial^2 \phi_2}{\partial x^2} - \Sigma_2 \phi_2 + p \Sigma_1 \phi_1 = \frac{1}{v_2} \frac{\partial \phi_2}{\partial t} \tag{20}$$

The subscript 1 refers to the high energy group and the subscript 2 to the low energy group. These equations are valid for the region outside the reactor core where there is no source of fast neutrons. Σ_1 is not an absorption cross section but rather, a removal cross section. Since the removal of neutrons from the high energy group

is primarily due to neutron moderation into the low energy group, the value to be used for Σ_1 may be based on the rate of thermalization in the medium and may thus be related to the neutron age and diffusion properties of the medium by: [3] [4] [22]

$$\Sigma_1 = \frac{D_1}{\tau} \tag{21}$$

where τ is the neutron age involved in slowing down from fission energies to thermal energies. Any absorption that occurs in the thermalization of the high energy neutrons is accounted for by the resonance escape probability, p , in the source term of equation (20). The value of p is unity in all common moderator materials.

If the low energy group is chosen as those neutrons which are in thermal equilibrium with the diffusion medium, (thermal group), and the fast neutron group as those which are above thermal energies, the group constants which have been determined for reactor design problems using two group diffusion theory may be utilized. These group constants, which are in general use, have been tabulated for the more common materials used as a diffusion medium surrounding a reactor core. [1] [3] [22]

Necessary boundary conditions for equations (19) and (20) are that both ϕ_1 and ϕ_2 are continuous and finite throughout the medium and both functions are continuous across the core-diffusion medium

interface. These boundary conditions may be used to obtain steady solutions to the two group diffusion equations where $\frac{\partial \phi}{\partial t} = 0$ in both equations (19) and (20). These solutions are:

$$\phi_1(x) = \phi_{10}\, e^{-\left[\frac{1}{\tau}\right]^{\frac{1}{2}}(x - x_0)} \tag{22}$$

$$\phi_2(x) = \left[\phi_{20} - F\,\phi_{10}\right] e^{-\left[\frac{\Sigma_a}{D_2}\right]^{\frac{1}{2}}(x - x_0)} + F\,\phi_{10}\, e^{-\left[\frac{1}{\tau}\right]^{\frac{1}{2}}(x - x_0)} \tag{23}$$

where

$$F = \frac{\frac{D_1 p}{D_2 \tau}}{\frac{\Sigma_a}{D_2} - \frac{1}{\tau}} \tag{24}$$

$$\phi_1(x) = \phi_{10} \text{ and } \phi_2(x) = \phi_{20} \text{ at } x = x_0.$$

It is apparent that equation (19) is of the same form as equation (2). If a solution exists in the form of equation (3), the values of the constants for the fast group, b_1 and a_1, are analogous to b and a of equations (17) and (18).

$$b_1 = \left[\frac{1}{\tau} + \frac{\omega^2}{4 D_1^2 v^2}\right]^{\frac{1}{2}} \tag{25}$$

$$a_1 = -\frac{\omega}{2 v_1} \frac{[\tau]^{\frac{1}{2}}}{D_1} \quad . \tag{26}$$

The fast group average velocity, v_1, appearing in equations (25) and (26) is difficult to determine since the velocity distribution is a function of both the slowing down distribution in the diffusion medium and of the energy spectrum of the fast group neutrons entering the medium from the reactor core. If the average velocity of the neutrons in the fast group is assumed to be $1.4 \times 10^7 \ \frac{cm}{sec}$, which corresponds to a neutron energy of only one hundred electron volts, representative values of a_1 and b_1 may be calculated for materials which are commonly used as diffusion media.

The results for such calculations with ω equal to five hundred radians per second are shown in Table 1 for water, heavy water, beryllium, and carbon. Frequencies over five hundred radians per second would be of little interest except for reactors with very short neutron lifetimes.

Table 1 also lists each of the two terms in equation (25) as well as the values of the fast group constants necessary for this calculation. It is apparent from the values in Table 1 that the second term in equation (25) is negligible compared to the first and that the value of b_1 is therefore not significantly different from the

TABLE 1

HIGH ENERGY GROUP PHASE SHIFT AND ATTENUATION CALCULATIONS* FOR DIFFUSION IN COMMON MODERATING MATERIALS

Material	τ, cm^2	D_1, cm	$\frac{1}{\tau}$, cm^{-2}	$\frac{\omega^2}{4 D_1^2 v_1^2}$, cm^{-2}	b_1, cm^{-1}	a_1, cm^{-1}
H_2O	31.4	1.143	3.18×10^{-2}	5.85×10^{-9}	0.1785	8.76×10^{-5}
D_2O	125	1.13	8.00×10^{-3}	2.34×10^{-8}	0.0894	1.76×10^{-4}
Be	97.2	0.63	1.06×10^{-2}	4.10×10^{-8}	0.1015	2.78×10^{-4}
C	364	1.11	2.75×10^{-3}	6.91×10^{-8}	0.0524	3.07×10^{-4}

* Calculations are for a frequency of five hundred radians per second and an average neutron velocity of 1.4×10^{-7} centimeters per second.

steady state attenuation exponent for the fast group used in equation (22). The calculated values for a_1 show that the phase shift for fast neutrons is negligible unless extremely large distances are considered. This calculation illustrates, then, that the actual velocity of the neutrons in the high energy group need not be accurately known as long as the average neutron energy is of the order of one hundred electron volts or greater.

Diffusion of neutrons in the thermal energy group, however, contributes a very significant phase shift to the neutron variation. Equations (17) and (18) may be used for a sample calculation. For a frequency of five hundred radians per second and water at twenty five degrees centigrade as the diffusion medium, the calculated values would be:

$$b_{th} = \left[0.120 + 0.00032\right]^{\frac{1}{2}} = 0.347 \text{ cm}^{-1} \tag{27}$$

$$a_{th} = 1.78 \times 10^{-2} \text{ radians per centimeter.} \tag{28}$$

The thermal group constants used for this calculation were:

$$E_a = 0.0195 \text{ cm}^{-1}$$

$$D_2 = 0.16 \text{ cm}$$

The average velocity for neutrons in thermal equilibrium with the medium at twenty five degrees centigrade was calculated to be

2.5×10^5 centimeters per second for a Maxwellian distribution.

From the above calculations it is apparent that although the attenuation of the neutron variation in water is not significantly different from the attenuation of the steady state component, the phase shift to be expected from a pure thermal flux is quite large for moderate distances from the core.

The measured thermal neutron variation at any spatial point, x_j, is composed of two components. One component consists of neutrons which have diffused through the medium as thermal neutrons from a previous point, x_{j-1}, to the point x_j, while the other consists of neutrons which have diffused through the medium as fast neutrons but have been reduced to thermal energies at x_j. The phase shift and amplitude of the measured variation are determined by the phases and amplitudes of these two components. The system output is the measured neutron variation divided by the steady state neutron level at x_j.

Let $A_j \cos \{\omega t + \theta_c + f(x)\}$ represent the component of the neutron variation arriving at the point x_j by thermal diffusion and $B_j \cos \{\omega t + \theta_c\}$ represent the component arriving by fast diffusion and slowing down. The measured variation will be proportional to the sum of these two components.

$$A_j \cos \{\omega t + \theta_c + f(x)\} + B_j \cos \{\omega t + \theta_c\}$$

$$= C_j \cos \{\omega t + \theta_c + a_j\} \tag{29}$$

where

$$\tan^{-1} a_j = \frac{A_j \sin f(x)}{B_j + A_j \cos f(x)} \tag{30}$$

$$C_j = A_j \cos a_j + B_j \cos \{f(x) - a_j\} \tag{31}$$

If $A_j \leqslant B_j$ and f(x) is less than ten or fifteen degrees, then excellent approximations are that:

$$a_j = \frac{A_j}{B_j + A_j} f(x) \tag{32}$$

$$C_j = A_j + B_j . \tag{33}$$

The function f(x) is the value of the phase shift per centimeter for thermal neutrons, a_{th}, calculated from equation (18), times the distance the thermal neutrons have diffused to reach the point x_j. In order to account for the various distances traveled, the following expression is proposed:

$$a_j = \sum_{m=1}^{j} \frac{A_m e^{-\left[\frac{\Sigma_a}{D_{th}}\right]^{\frac{1}{2}}(x_j - x_m)}}{B_m + A_m e^{-\left[\frac{\Sigma_a}{D_{th}}\right]^{\frac{1}{2}}(x_j - x_m)}} a_{th}(x_m - x_{m-1}). \qquad (34)$$

In this manner, the thermal neutrons from the points more distant from x_j than x_{j-1} are given a weighting according to the probability that they will arrive at x_j. The weighting factor is applied to the thermal diffusion terms only. It is apparent that this expression reduces to the one group model proposed earlier for the case where $B_m = 0$.

$$a_j = \sum_{m=1}^{j} a_{th}(x_m - x_{m-1}) = a_{th}(x_j - x_0). \qquad (35)$$

This expression for thermal neutron diffusion only is to be expected since all neutrons arriving at x_j have diffused as thermal neutrons from x_0.

Appropriate values for the constants A_m and B_m may be inferred from an examination of the thermal group diffusion equation, equation (20). A_m is proportional to the product of the thermal diffusion coefficient and the amplitude of the second derivative of the thermal

flux variation evaluated at x_m. B_m is proportional to the product of the fast diffusion coefficient and the amplitude of the fast flux variation evaluated at x_m divided by the age, τ.

$$A_m = D_{th} \left. \frac{\partial^2 \left[\Delta\phi_{cth} \, e^{-b_{th}(x - x_0)} \right]}{\partial x^2} \right|_{x=x_m} \tag{36}$$

$$B_m = \frac{D_1}{\tau} \, \Delta\phi_{cl} \, e^{-\left[\frac{1}{\tau}\right]^{\frac{1}{2}} (x - x_0)} \Bigg|_{x=x_m} . \tag{37}$$

For the particular case where the diffusion medium is water, it can be shown that equation (17) reduces to

$$b_{th} = \left[\frac{\Sigma_a}{D_2}\right]^{\frac{1}{2}} , \tag{17a}$$

since the last term is negligible as seen in equation (27).

From equation (8)

$$\frac{\Delta\phi_{th}}{\phi_{th\,0}} \qquad \frac{\partial^2 \phi_{th}(x)}{\partial x^2} = \frac{\partial^2 \left[\Delta\phi_{c\,th} \, e^{-b_{th}(x - x_0)} \right]}{\partial x^2} \tag{38}$$

or

$$A_m = D_{th} \frac{\Delta\phi_{c\,th}}{\phi_{th\,0}} \frac{\partial^2\phi_{th}(x_m)}{\partial x^2} \tag{39}$$

where $\phi(x_m)$ indicates that the function is to be evaluated at x_m.

Also, using equation (22):

$$B_m = \frac{D_1 \Delta \phi_{c\,1}}{\phi_{10}} \phi_1(x_m) \tag{40}$$

but since it was assumed that the point model kinetic equations were valid in the core, the ratio of the fast to thermal flux in the core must remain constant and:

$$\frac{\Delta\phi_{c\,1}}{\phi_{10}} = \frac{\Delta\phi_{c\,th}}{\phi_{th\,0}} \tag{41}$$

Substituting (39) and (40) into equation (34) and making use of equation (41):

$$a_j = \sum_{m=1}^{j} \frac{D_{th} \frac{\partial^2\phi_{th}(x_m)}{\partial x^2} e^{-\left[\frac{\Sigma_a}{D_{th}}\right]^{\frac{1}{2}}(x_j - x_m)}}{\frac{D_1}{\tau}\phi_1(x_m) + D_{th}\frac{\partial^2\phi_{th}(x_m)}{\partial x^2} e^{-\left[\frac{\Sigma_a}{D_{th}}\right]^{\frac{1}{2}}(x_j - x_m)}} a_{th}(x_m - x_{m-1}). \tag{42}$$

Equation (42) will probably be a good approximation for materials other than water but experimental verification should be made. It was not possible to evaluate materials other than water in the experimental work described in this paper.

The value of C_j may be calculated from equation (31) or, if a_j is small, from equation (33). The value of C_j is a relative value and may be used to calculate the change in the amplitude of the variation as a function of position. The ratio of the amplitude of the variation to the steady state neutron concentration at x_j may be obtained by normalizing C_j to the value of this ratio at $x = x_0$.

$$\frac{\Delta n(x_j)}{n(x_j)} = \frac{C_j}{C_0} \quad \frac{\Delta \phi_{c\ th}}{\phi_0}, \tag{43}$$

where

$$C_0 = A_0 + B_0 = D_{th} b_{th}^2 \Delta \phi_{c\ th} + \frac{D_1}{\tau} \Delta \phi_{c\ 1}. \tag{44}$$

The response measured at some detector location x_j as a function of frequency may then be related to the reactor response by

$$\theta_r = \theta_j - a_j \tag{45}$$

$$\frac{\Delta n}{n_0} = \frac{\Delta n(x_j)}{n(x_j)} \quad \frac{C_0}{C_j} \tag{46}$$

where

θ_r = the phase of the reactor response relative to the reactivity input

θ_j = the phase measured at x_j relative to the reactivity input

$\frac{\Delta n}{n_0}$ = the relative amplitude of the reactor response

$\frac{\Delta n(x_j)}{n(x_j)}$ = the relative amplitude measured at x_j.

Experimental Verification

The model developed in the preceding section can be tested by experimental measurements. Of particular interest is the expression for the phase shift as a function of position in the diffusion medium, equation (42). Accurate determination of the phase and amplitude of the neutron variation in the medium when the reactor core is forced in a sinusoidal manner is required at several points. Relative values of the spatial distribution of both the high energy and the low energy neutron flux are also required to evaluate the terms that appear in equation (42).

If ϕ_{th} and ϕ_1 are accurately determined then the calculated value of a_j from equation (42) may be compared with the experimental measurements.

It is to be expected that the steady state spatial flux distributions are not accurately described by the equations (22) and (23) since the geometry of the reactor, employed for the experimental work, is not as simple as that implied by the approximation used to obtain these equations. The second derivative required in equation (42) can be obtained experimentally from the measured spatial distribution of the thermal flux. From this measurement, then:

$$\left.\frac{\partial^2 \phi_{th}(x)}{\partial x^2}\right|_{x=x_j} = \frac{\dfrac{\phi_{th}(x_{j-1}) - \phi_{th}(x_j)}{x_j - x_{j-1}} - \dfrac{\phi_{th}(x_j) - \phi_{th}(x_{j+1})}{x_{j+1} - x_j}}{\frac{1}{2}(x_{j+1} - x_{j-1})} . \qquad (47)$$

CHAPTER IV

EXPERIMENTAL EQUIPMENT

The Nuclear Reactor

The experimental work done to support the theoretical considerations was performed on the University of Oklahoma AGN-211 nuclear reactor. A photograph of the top of the reactor core and surrounding region is shown in Figure 1.

The reactor is a compact, hydrogen-moderated system utilizing enriched uranium fuel. The uranium, enriched to 20 per cent U^{235}, is in the form of a fine powder of UO_2 dispersed in polyethylene fuel elements. Twelve uranium bearing plastic blocks approximately three inches square and ten inches high comprise the central core region of the reactor. Since only a one-eighth inch, water-filled gap exists between the fuel elements, the system is very well approximated by assuming a homogeneous core region.

A graphite reflector completely surrounds the core but is not of uniform thickness. The graphite is five inches thick on the top and bottom, six inches thick on each side and three inches thick on the front and rear faces. Since the entire reactor assembly is suspended near the bottom of a water filled tank thirty-nine inches wide by

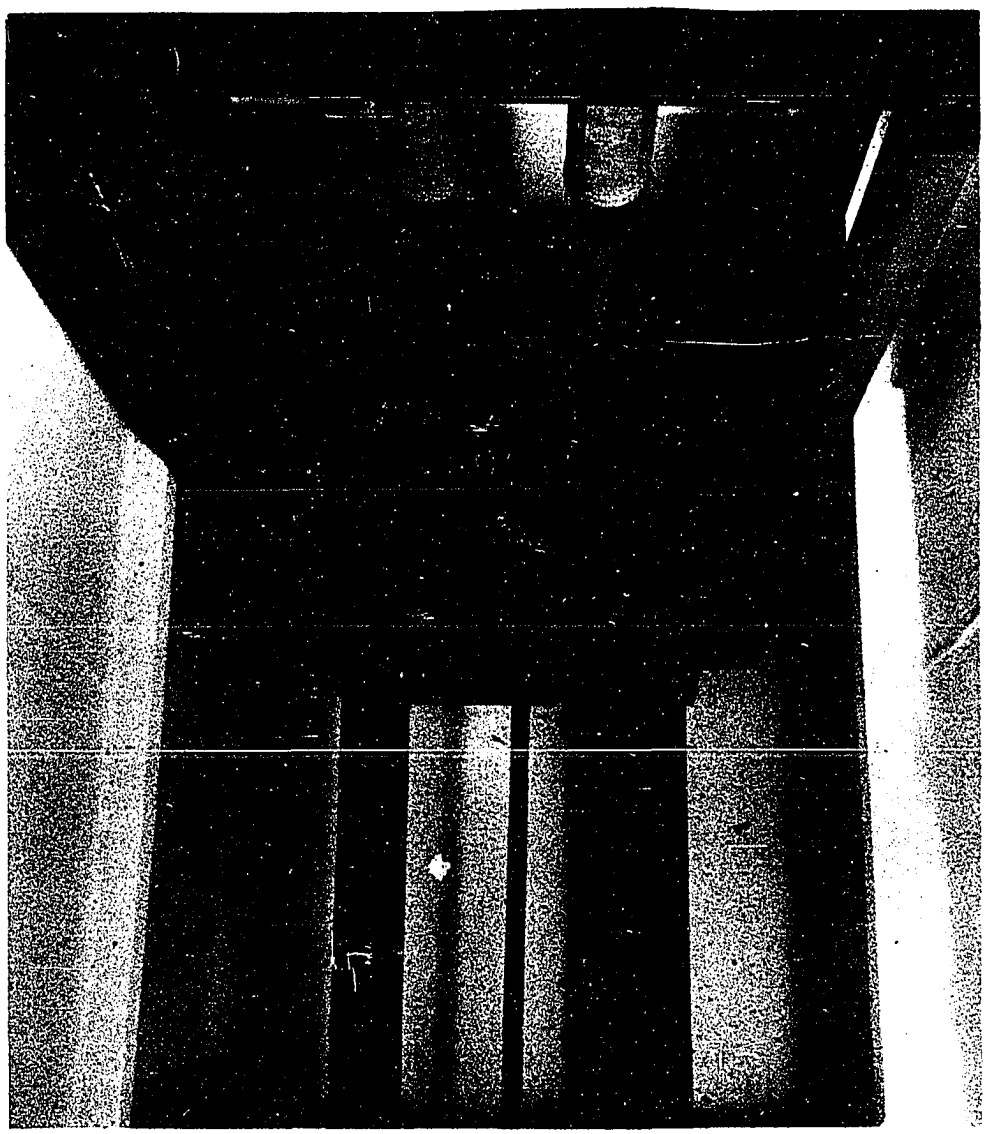

TOP VIEW OF AGN-211 REACTOR

FIGURE 1

fifty-nine inches long by ninety-six inches deep, a second reflector of water surrounds the graphite reflector. The water serves as a radiation shield as well as a reflector.

Experimental facilities are provided in the form of a central access tube seven-eights of an inch inside diameter extending horizontally through the center of the core, a reflector port of four inches inside diameter extending through the six inch side reflector at the reactor center plane and a four inch beam port abutting the reflector on the side opposite the reflector port. Also, the reactor is located near one end of the tank so that a water region of twenty-nine inches is available adjacent to the front face of the reactor for experimental purposes. The experimental ports extend through this water region, on through the concrete shield surrounding the tank, and open into the experimental area at the west reactor shield face. A plan view showing the relative location of the reactor and facilities is shown in Figure 2.

Four control rods are provided for safety and control of the reactor. These are the flat blades seen above the core in Figure 1. Two of these rods must be withdrawn completely from the core and are for safety purposes only. One other, the coarse control rod, was also completely withdrawn for all of the present experimental work.

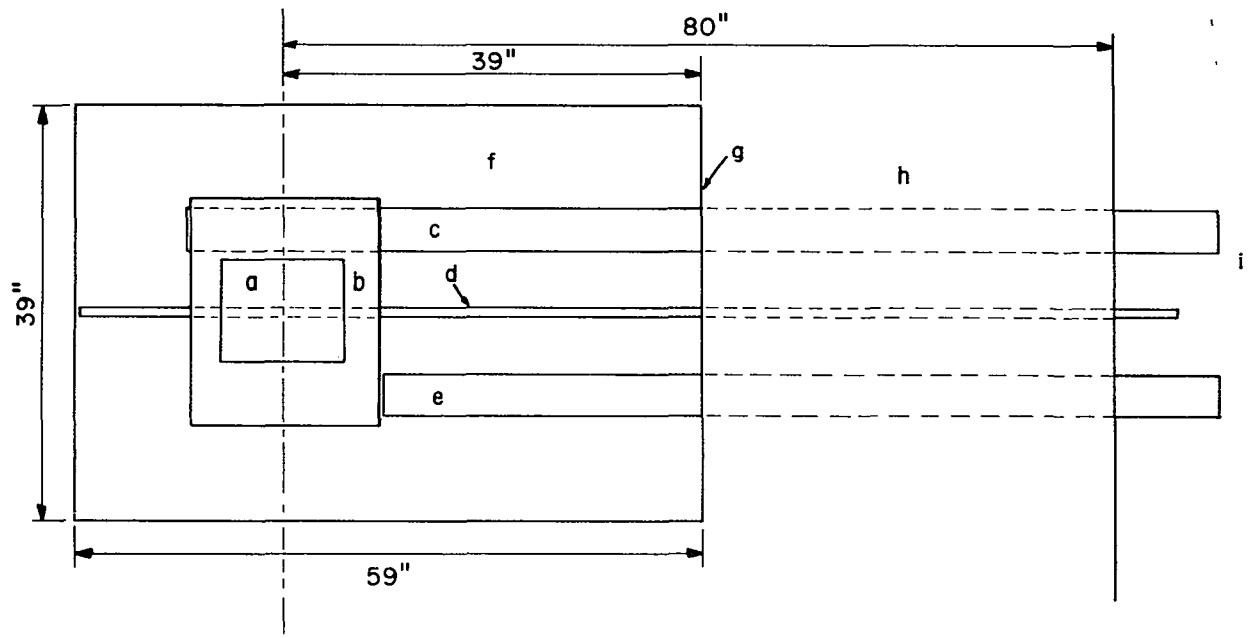

PLAN VIEW OF REACTOR AREA

KEY TO PLAN VIEW OF REACTOR AREA

a. Reactor core
b. Graphite reflector
c. Reflector port
d. Central access tube
e. Beam port
f. Water reflector and shield
g. Tank wall
h. Concrete shield
i. Experimental area

FIGURE 2

The fourth is the fine control rod and is used to compensate for small reactivity changes during operation to insure stable operating conditions. All rods are located several neutron mean free paths from any of the experimental equipment installed in the reactor during operation so that interaction of the control rods with the experiment was negligible.

Three neutron monitors are permanently installed adjacent to the core and are used to monitor average operating level. The time constants associated with this instrumentation are such that good average readings may be obtained for the frequencies used in the experimental work.

Input Signal Generator

The generator for the input signal to the reactor consisted of an oscillator rod capable of changing the reactivity of the reactor in a sinusoidal manner when rotated with uniform angular velocity. This oscillator rod was constructed of polyethylene with a partial covering of cadmium and was inserted into the reflector port adjacent to the reactor core. A photograph of the oscillator rod is shown in Figure 3.

The rotor portion of the oscillator rod was a three and one-half inch diameter polyethylene cylinder six inches long. It was mounted on a steel shaft which was supported in ball bearings mounted in polyethylene bearing support plates. These support plates were of

OSCILLATOR ROD

FIGURE 3

such a diameter as to provide a snug fit in the reflector port. A clamp which could be tightened after the oscillator rod was inserted prevented the outer bearing support plate from moving and insured that the effect of the oscillator rod did not change due to a change in position.

A cadmium strip was placed partially around the cylinder at the end nearest the reactor center. This strip was one and one-half inches wide and long enough to cover approximately one half of the circumference of the cylinder. The length of the strip and the shape of the ends were adjusted to give a good sinusoidal input when the cylinder was rotated. Four different modifications in strip shape were evaluated to arrive at the final shape. Subsequent analysis of the oscillator calibration showed that the final curve could be described by a fundamental plus a two per cent second harmonic. Since all data were to be obtained with the same input, this amount of harmonic content was considered acceptable.

Attached to the outer end of the cylinder was a small permanent magnet which was used to induce an electrical pulse in a pickup coil mounted on the outer bearing support. This pulse was used in connection with the data accumulation equipment to establish a phase reference point. Lead foil was used as counterbalances for both the

cadmium strip and the magnet.

A seven foot shaft connected the oscillator rod to the external drive motor outside the reactor shield. Bearing supports were provided at one foot intervals so that the oscillator could be driven at high frequencies.

The oscillator rod was inserted into the reflector port as near the reactor center as practical. It was not possible to center the cadmium strip since the excess reactivity of the reactor was too low for operation unless a portion of the reflector port inside the reflector was filled with a graphite plug. The excess length of polyethylene served as an additional reflector outside the cadmium. Any closer positioning of the cadmium toward the center would have prevented calibration of the oscillator rod over a full revolution. The reactivity would have been negative, even with all of the control rods withdrawn, when the cadmium was adjacent to the core. A section drawing of the facility showing the location of the oscillator rod relative to the core is shown in Figure 4.

The oscillator rod drive consisted of an 1800 RPM synchronous motor and fixed gear ratio speed changers. A variable speed reduction drive was available but was not used extensively since the constant frequency required could not be achieved over the length of

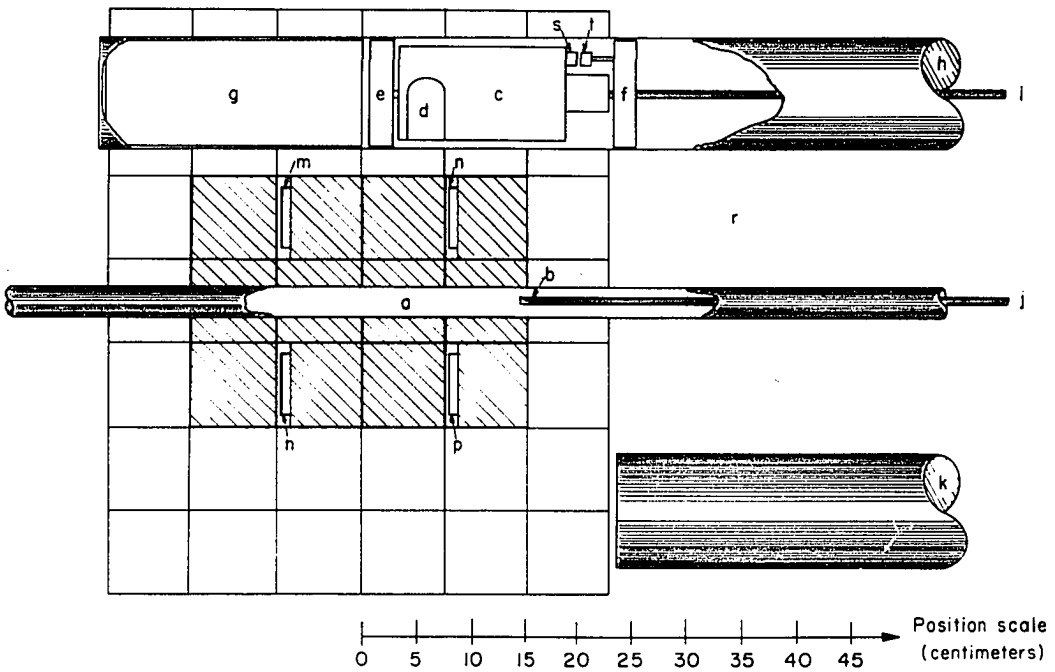

SECTION VIEW OF REACTOR CORE REGION

KEY TO SECTION VIEW OF REACTOR CORE REGION

a. Central access tube
b. Fission counter output detector
c. Polyethylene oscillator rod
d. Cadmium strip input generator
e. Rear bearing support plate
f. Front bearing support plate
g. Graphite plug
h. Reflector port
i. Oscillator rod drive shaft
j. Fission counter signal lead
k. Beam port
m. Fine control rod guide
n. Safety rod guides
p. Course control rod guide
r. Water experimental region

FIGURE 4

time necessary for data accumulation. The fixed gear ratios used were factors of two and ten. The basic motor frequency of 30 cycles per second could thus be changed to 1.5, 3, 6, 15 and 60 cycles per second with proper arrangement of the gears, which proved to be an adequate number of frequencies for experimental purposes. The location of the drive motor is shown in Figure 5. This photograph also shows the relative location of the experimental facilities in the test area outside the concrete shield. The locations of the test area and experimental facilities relative to the core are indicated on the area plan view in Figure 2.

Output Detector

The output signal required for the experimental program is the time dependent variation of the number of neutrons per cubic centimeter at several spatial points. The neutron detector used was a small flux mapping fission counter, Westinghouse type 7186. This counter is built into the end of a long tube which serves as the outer jacket of the counter and as the outer shield for the signal lead used to transmit the detector signal to the test area. The stainless steel tube has an outside diameter of one-fourth inch and a wall thickness of approximately 0.012 inches. In the sensitive detector region the inside surface of the tubing is coated with highly enriched uranium. This coating, which

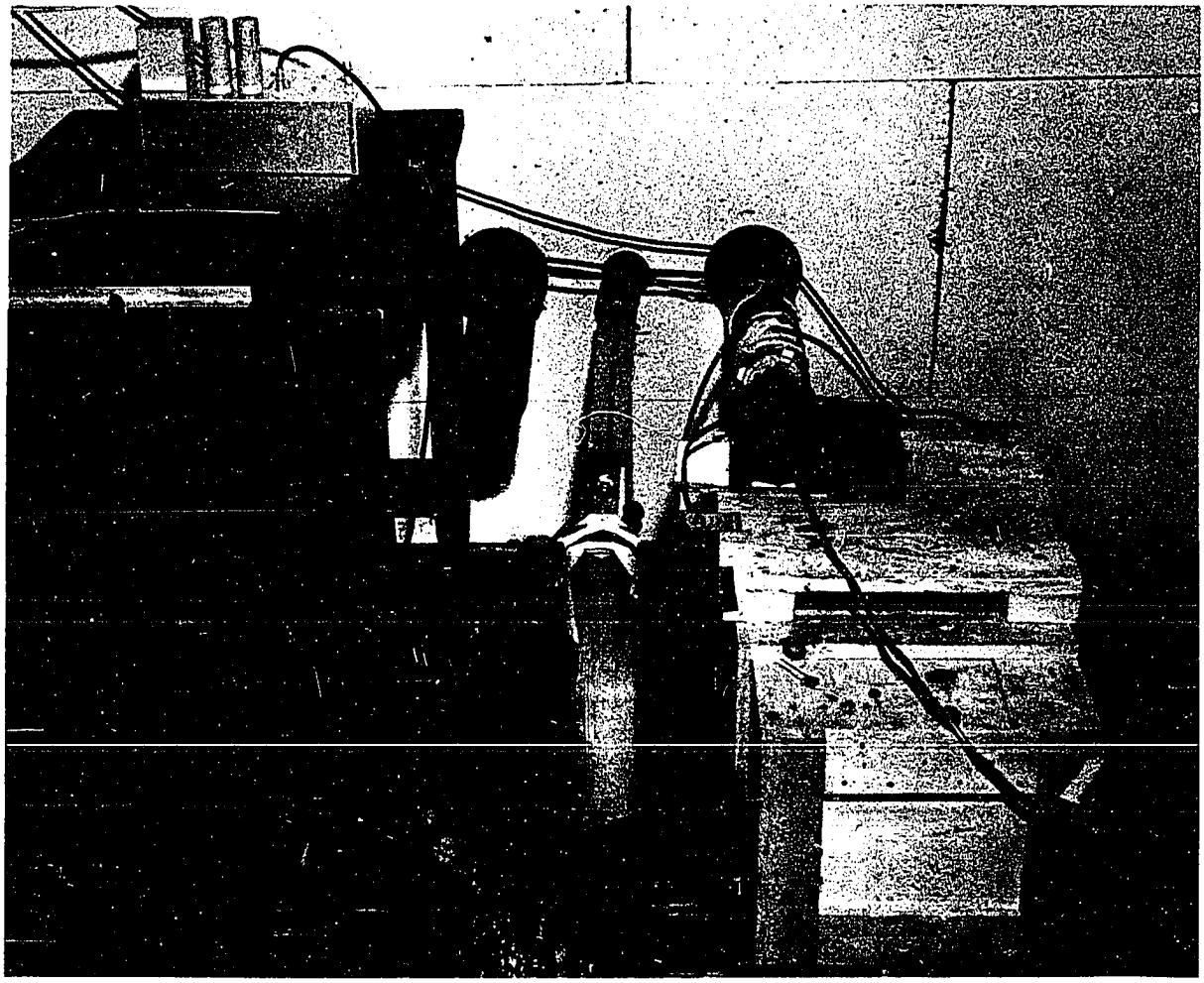

EXPERIMENTAL AREA AND SHIELD FACE

FIGURE 5

extends over a length of three-eighths of an inch, contains 0.0017 grams of U^{235}. The entire tube is filled with an argon-nitrogen gas mixture. Energetic fission fragments, produced by neutron induced fission of the U^{235} in the coating, ionize the gas to produce a current pulse if a voltage is applied to the central electrode.

Since the fission cross section is over 500 barns at thermal neutron energies and drops to a few barns at energies above thermal, [28] nearly all of the fission induced pulses are caused by thermal neutrons. To a very good approximation, then, the detector output in the form of number of pulses per unit time is proportional to the thermal neutron concentration at the position of the sensitive part of the detector. Since all relations involving neutron concentrations in the kinetic study involve ratios of the variation of the neutron concentration to the average value, it is not necessary to know the absolute sensitivity of the detector.

The stainless steel tube is of sufficient length that the sensitive portion of the detector may be located in any portion of the reactor core or surrounding reflector. For this experimental work the detector was in the central access tube passing through the reactor center. A coaxial cable connector mounted on the end of the tube allowed the pulse to be transmitted to a pulse amplifier. The end of

the detector tube, the coax cable and the pulse preamplifier appear in Figure 5.

During operation the detector was encased in a thick polyethylene sleeve. A polyethylene rod three-fourths of an inch in diameter and three feet long was drilled axially to accept the detector with the sensitive portion at the center of the rod. This polyethylene insured that neutrons did not travel directly down the access tube to the detector. Also, since polyethylene has nearly the same hydrogen atom density as water, the polyethylene filling of the access tube reduced the discontinuity in the water otherwise present.

Data Accumulation

A photograph of the equipment used to accumulate the experimental data is shown in Figure 6. The instruments shown in the left half of the photograph are those used specifically for this experimental program while the console on the right is the reactor control center. The instruments in the console are used primarily for reactor control but also provide information required for this experimental program. The instrumentation on the left provides for the accumulation, recording and preliminary analysis of the time dependent reactor output. It also includes calibration and testing equipment to insure valid output data. A block diagram of this portion of the instrumentation is shown in Figure 7.

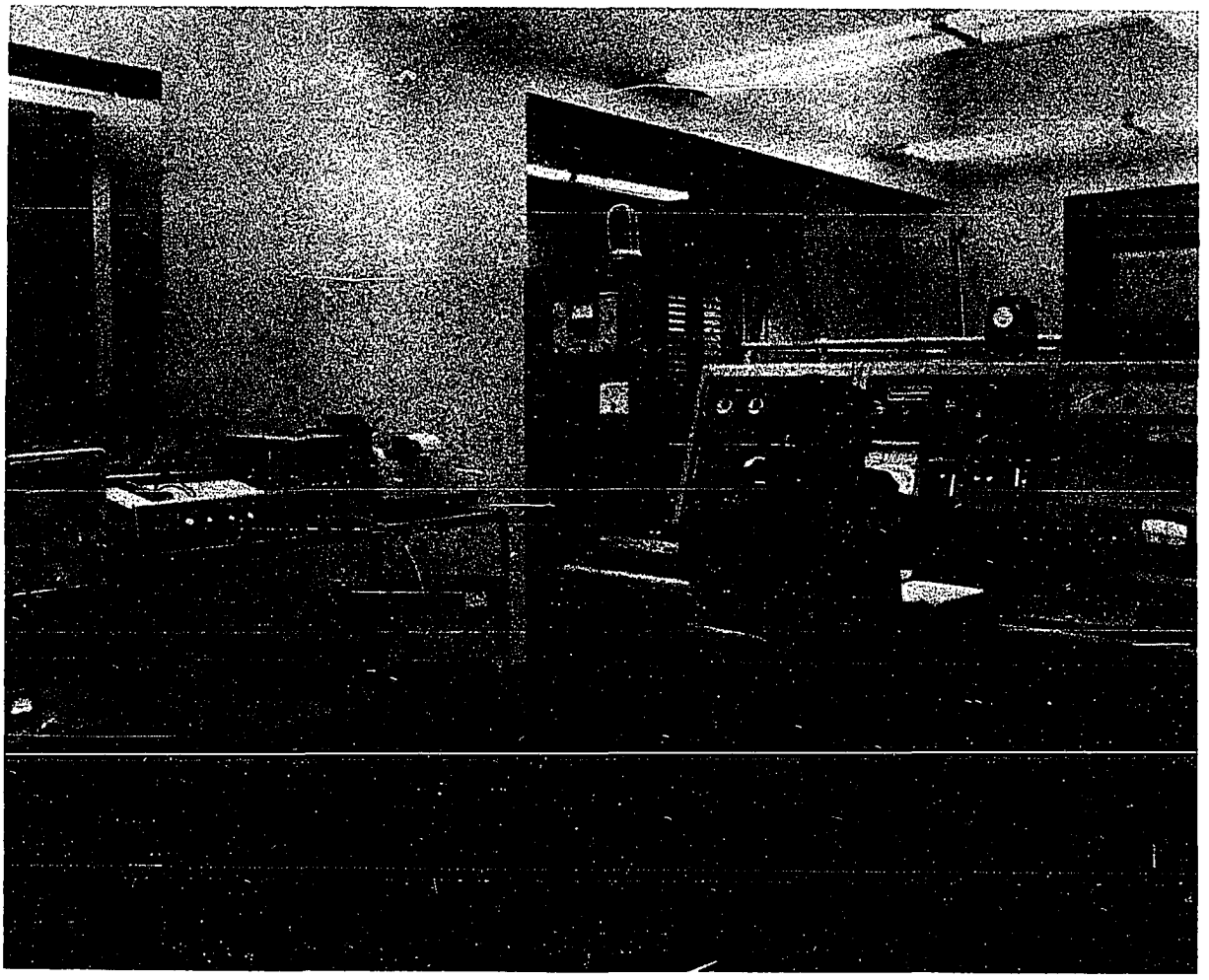

DATA ACCUMULATION INSTRUMENTATION

FIGURE 6

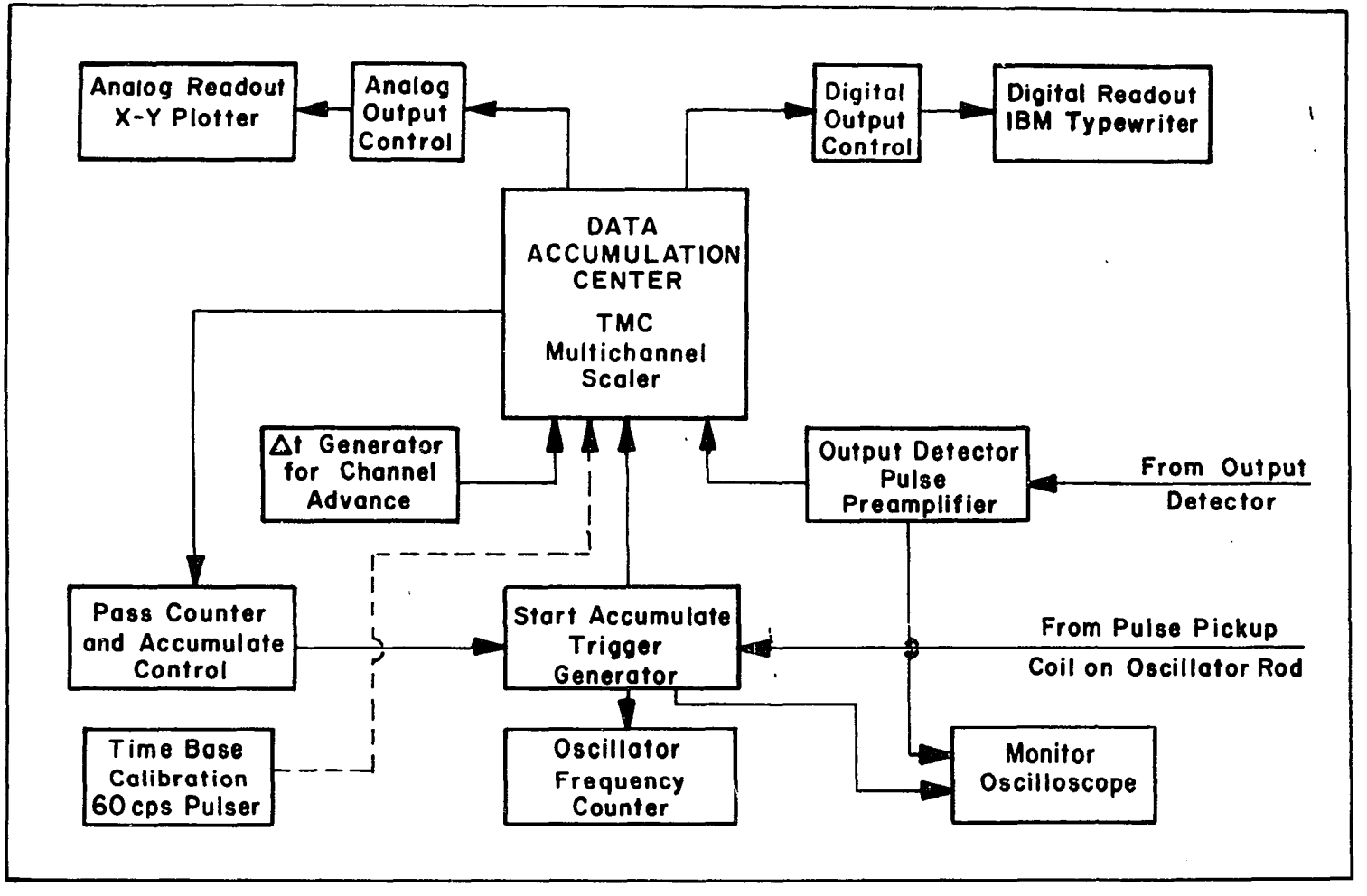

BLOCK DIAGRAM OF DATA ACCUMULATION INSTRUMENTATION

FIGURE 7

The center of the data accumulation instrumentation was a Technical Measurements Corporation Multichannel Analyzer, type 402, operated in the multiscaler mode. In this mode of operation input pulses above a selected threshold were counted into memory channels sequentially following a "start accumulate" signal. The threshold was set so that noise pulses were not counted. The number of sequential channels to be used may be 100, 200, or 400. Each channel is capable of storing up to 100,000 pulses. The length of time that a channel was open to accept pulses was determined by a timing pulse supplied either internally from a built in timer or externally from the Δt generator for channel advance.

The sequence of events which occurred when the accumulate control on the pass counter was energized was:

1. The first pulse received by the start accumulate trigger generator from the pulse pickup coil on the oscillator rod reset the channel selection in the multichannel scaler to zero.
2. The first pulse received from the Δt generator after this caused the scaler to begin accumulation of pulses from the output detector in channel zero.
3. The next Δt generator pulse caused the multichannel scaler to advance the channel selector to channel one and again accumulate pulses from the output detector for a time equal to Δt.

4. The channel advance continued with each Δt pulse until the preselected number of channels had been utilized. (Usually 100 channels were used.) This channel advance is not interrupted by the arrival of start accumulate trigger pulses while it is in progress.

5. The full sweep across all channels used is referred to as one "pass". Following a pass, which was counted on the pass counter, all accumulation stopped.

6. The next pulse from the pulse pickup coil following the end of the first pass initiated the cycle again and another pass was completed and counted.

7. This accumulation continued until either the preset limit on the pass counter and accumulate control was reached or until a sufficient number of counts had been accumulated in each channel and the run was terminated manually.

8. The data, now stored in the memory unit of the multichannel scaler, could be read out either graphically or digitally by means of the appropriate readout.

It is apparent from the above sequence that each pass began at the same relative phase point of the input signal generator since it was initiated by a pulse from the phase reference pickup.coil. Thus the

information stored in the memory of the multichannel scaler represented the sum of many output measurements over selected intervals of time, the number of measurements being the number of passes made to accumulate the data.

The number of passes required is a function of the countrate from the output detector and the value of Δt selected. The value of Δt was chosen such that approximately one and one-half periods of the input signal were equal to Δt times the number of channels used. In this manner approximately one and one-half cycles of the output signal were observed.

For example, a value of Δt of 0.5 milliseconds was used for an input frequency of 30 cycles per second when 100 storage channels were programed. Thus, one pass took 50 milliseconds or 1.5 cycles of the signal. The countrate was limited to a maximum of 8,000 counts per second since higher countrates caused increased counting losses due to dead time of the output detector amplifier and the scaler. A curve showing the counting loss correction factor as a function of countrate is given in Figure 8. From this figure it is apparent that if the countrate could be always less than 2,500 counts per second, no count loss correction would be required. However, this restriction leads to excessively long data accumulation times as well be shown. Since the

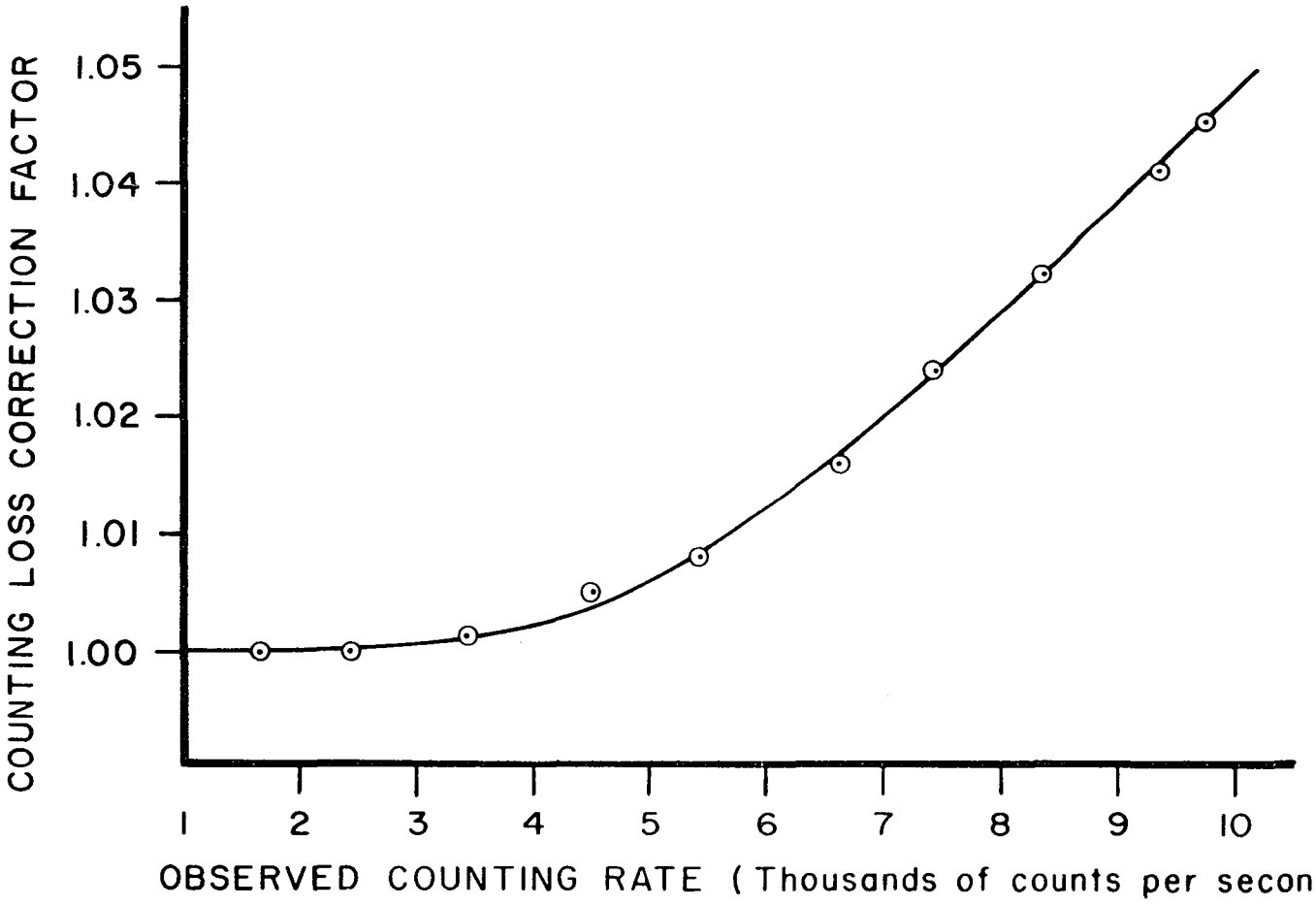

Neutron Detector Correction Factor as a Function of Observed Counting Rate

FIGURE 8

output signal was a statistically uncertain value, it was necessary to obtain a minimum of 50,000 counts in each channel to insure that the deviation would be low enough to yield the desired accuracy. It can be seen in this example, then, since Δt is 0.5 milliseconds, the countrate is 8,000 counts per second, and the total count is not less than 50,000 counts in each channel, that a minimum of 12,500 passes are required. Thus, it takes approximately thirteen minutes to obtain the data for one point at the maximum allowable countrate. It is apparent that the input frequency and the value of Δt must remain constant during this time if the output data is to be accurate. Since difficulty was encountered in maintaining a constant Δt within acceptable limits for more than thirty minutes, high countrates were used.

When the variable drive was used on the input signal generator the input frequency was determined by counting the pulses from the pulse pickup coil for a preset time on the oscillator frequency counter while the run was in progress. When the fixed gear ratios or direct drive were used with the synchronous motor, the signal from the pulse pickup coil was monitored on an oscilloscope in which the sweep frequency was synchronized with the 60 cycle line frequency. Any slipping of the shaft couplings or motor of only a few degrees was quickly apparent. The value of Δt was determined before and after each data run by the use of a reference 60 cycle pulser which was also synchronized with

the line frequency so that oscillator frequency and Δt were both referenced to the same base.

The form of the data obtained with this equipment is discussed in the following chapter.

CHAPTER V

DATA REDUCTION AND EXPERIMENTAL RESULTS

The experimental data obtained from the equipment previously described were in the form of an array of numbers representing the number of counts stored in each of the one hundred memory channels. A typical output page is shown in Table 2. The numbers were typed automatically by the analyzer and the headings were inserted manually to identify the data for subsequent analysis. It was also possible to obtain a graphical display of the data as shown in Figure 9 and Figure 10. This automatic graphing of the data with suppressed zero shows very clearly the statistical nature of the output data. It was felt that analysis of the graphical data would provide information concerning the amplitude and phase of the reactor output but sufficient accuracy could not be obtained from this approach. The graphical display did, however, serve a very useful purpose. Any severe noise conditions or malfunction of the equipment could be observed on the graphical display and the data rerun if unexpected variations were apparent. The graphical display was used as a visual monitor during the accumulation of data. The data in Figure 9 were obtained at an oscillator frequency of thirty cycles per

TABLE 2

REACTOR OSCILLATOR DATA

RUN 376
POSITION: 7.5 inches west of center
OSCILLATOR FREQUENCY: 6.0 cps
TIME PER CHANNEL: 1.876 milliseconds

51940	52139	51853	51767	51286	51208	51314	51018	50918	50898
50519	50803	50670	50916	50422	50384	50632	50231	50385	50699
50955	51447	51050	50956	51060	51233	51734	51649	51655	52075
51928	52710	52508	52596	53286	53558	54007	53702	54216	54554
54540	54947	55424	55140	55403	56164	55958	55974	56381	56465
56802	56706	56652	57148	57248	57228	57132	57509	57197	57963
57641	57815	57974	57112	51437	57585	57490	57154	56998	56817
56667	56333	56179	56370	55813	55666	55646	55239	54915	54515
54816	53950	54043	53543	51340	53374	52452	52715	52502	52088
52244	51750	51649	51547	51147	51250	51307	50796	51137	50621

RUN 392
POSITION: reactor center
OSCILLATOR FREQUENCY: 30 cps
TIME PER CHANNEL: 0.9579 milliseconds

41383	39803	39826	39442	38973	39193	39337	38979	39131	38653
38731	38573	38587	38586	38180	38319	37998	37802	38128	37988
37503	37352	37397	37146	31696	37568	37425	37562	37233	37483
37283	37631	37973	38068	37832	37761	37984	38032	38320	38292
38264	38518	38408	38685	38694	38737	39268	38984	38975	39806
39803	39561	39704	39983	40118	39654	39781	40171	40105	40076
39949	40388	40027	40075	40260	40325	40226	40373	39981	40230
39970	39978	39833	39748	39261	39707	39232	39184	38900	39028
38500	38408	38535	38466	38531	38433	37801	37636	37969	37535
37675	38139	37628	37496	37436	37504	37421	37519	37286	37366

RUN 382
POSITION: 17.0 inches west of center
OSCILLATOR FREQUENCY: 60 cps
TIME PER CHANNEL: 0.9574 milliseconds

54456	54918	54343	54212	53779	51772	51683	51178	51702	51241
51482	50960	50621	50620	50841	50790	50662	51251	51220	51252
53548	53451	53829	53966	54234	54319	54514	54934	55265	54960
55304	55700	55381	55234	55190	55309	54817	54944	54112	54644
54064	54101	53900	53390	51267	53332	52960	53179	52757	52333
53049	53322	52809	52533	53111	53444	53762	54169	53875	53915
54537	54679	54698	54725	51132	55260	55167	55377	55226	55009
54925	54998	54990	54411	54940	54114	54114	53465	53397	53371
53074	53090	52567	52704	51120	52994	52802	52855	53001	53192
53131	53525	53461	54252	54110	54437	54172	52122	54969	54826

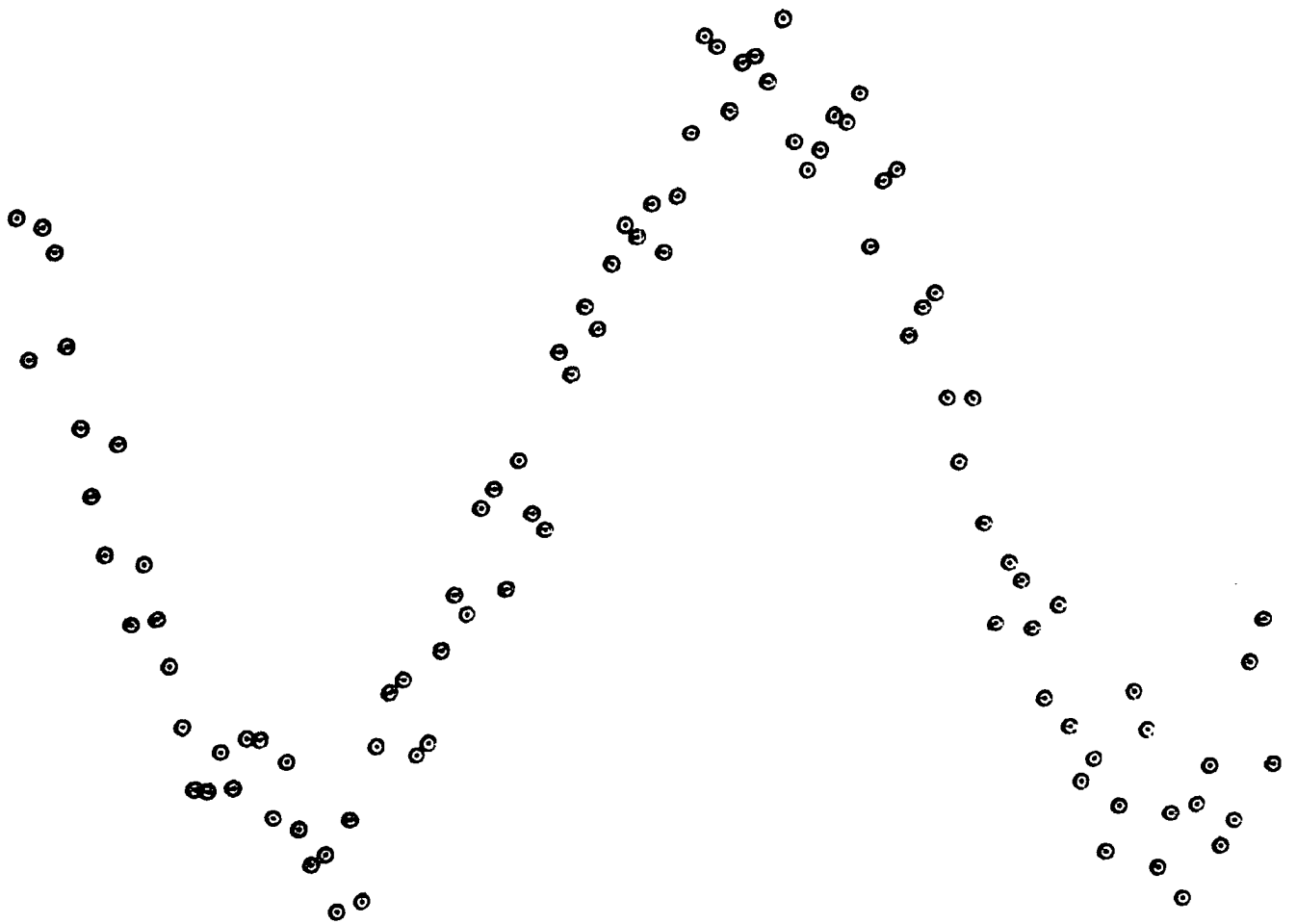

AUTOMATIC DATA PLOT, 30 CPS AT 48.2 CM.

FIGURE 9

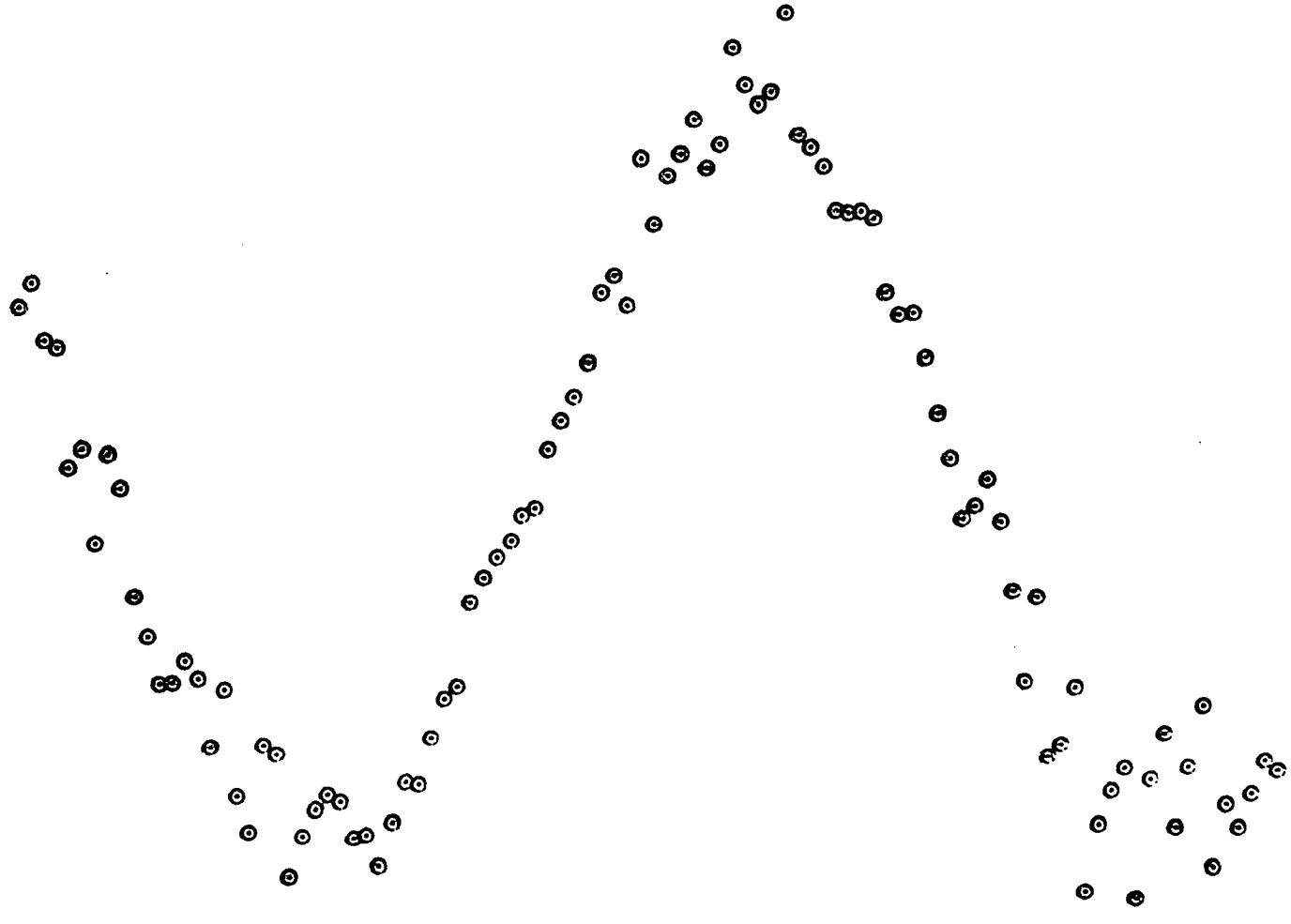

AUTOMATIC DATA PLOT, 30 CPS AT 23.0 CM.

FIGURE 10

second with the detector 48.2 centimeters from the reactor center. It is apparent that the data in Figure 9 are more scattered than those in Figure 10. The latter were obtained at the same oscillator frequency but with the detector only 23.0 centimeters from center. Subsequent analysis showed this observation to indeed be true--the variance of the data in Figure 9 being 1.4×10^5 while that for the data in Figure 10 was only 5.5×10^4. It is apparent that an indication of the relative worth of the data could be obtained from the graphical display but it was impossible to obtain an accurate indication of any phase shift between the two curves. The latter information must be obtained by digital analysis of the numerical data.

The first step in the analysis of the experimental data was to obtain, on an IBM 1410, a least square fit of the numerical data to the curve

$$y_n = A + B \cos(2\pi f n \Delta t) + C \sin(2\pi f n \Delta t) \qquad (48)$$

where f is the frequency of the oscillator rod, n is the channel number and Δt is the time each channel is open for the accumulation of data. From this fit the relative phase angle, θ, for the run was determined from

$$\theta = \tan^{-1} \frac{C}{B} . \qquad (49)$$

The ratio of the peak to peak amplitude of the sinusoidal variation

to the average value, A, was also determined. This ratio, $\frac{\Delta n}{n_o}$, is given by

$$\frac{\Delta n}{n_o} = 2\frac{(B^2 + C^2)^{\frac{1}{2}}}{A}. \tag{50}$$

The mean square error and the mean absolute error of the data relative to the computed curve were also calculated.

A portion of the curves resulting from two such calculations are shown in Figure 11 together with the experimental data points used to compute the values for the curves. The zero point on the curve is suppressed so that the derivation of the experimental data from the calculated curve is apparent. Zero suppression was accomplished by subtracting the computed value of A from each data point. Two curves, one with the oscillator rotating at 3.0 cycles per second and the other at 30.0 cycles per second are shown. The value of Δt for each run was such that about one cycle is displayed although 100 channels comprising about 1.5 cycles were used for the calculation. The detector was located 23.0 centimeters from the reactor center for both sets of data. The increased phase shift and attenuation at the higher oscillator frequency are apparent.

The relative phase, θ, calculated from the data is an indication of the phase of the reactor output relative to trigger point established by the angular location of the trigger pickup coil on the oscillator rod

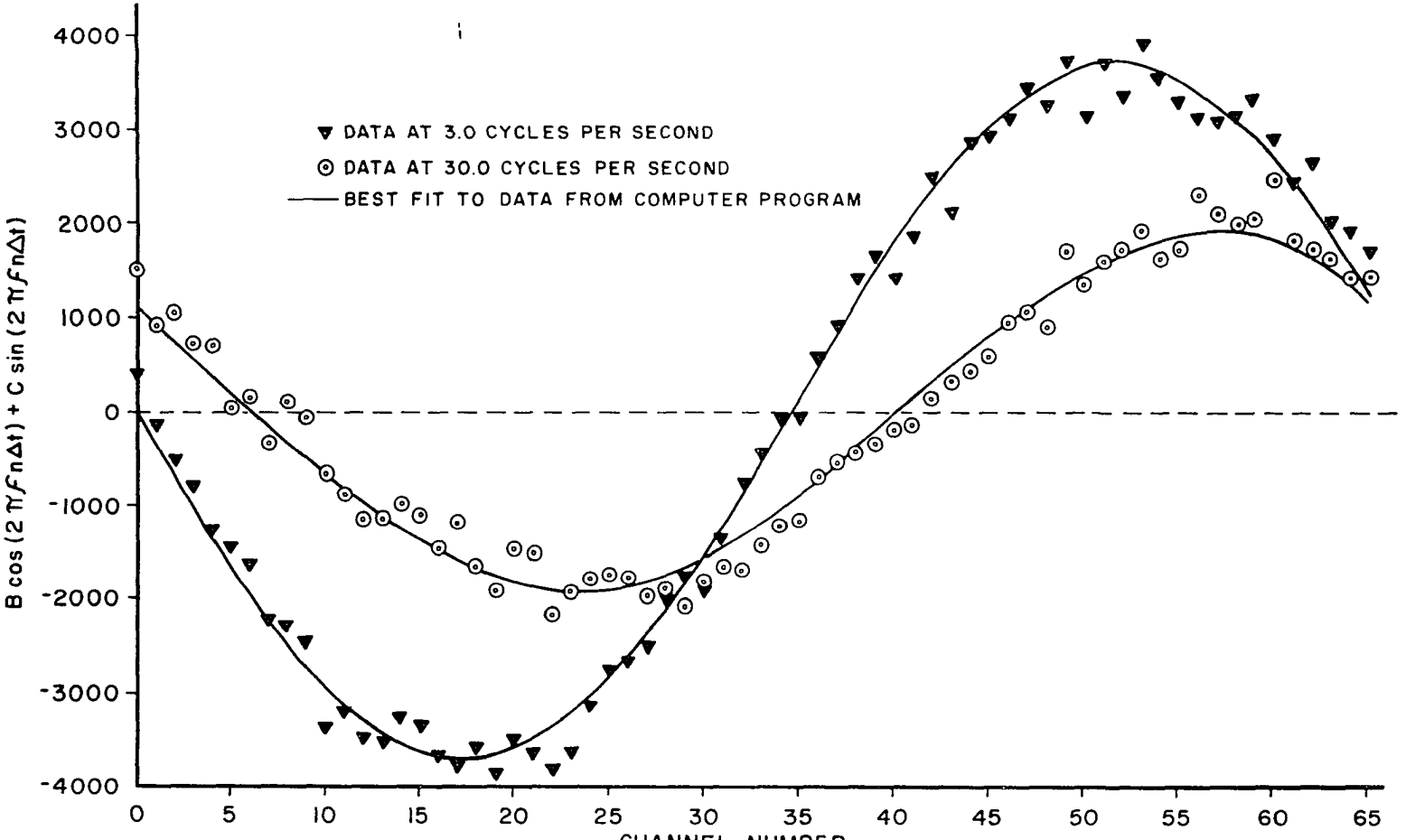

Results of Computer Curve Fitting Program

FIGURE 11

bearing support. This location cannot be determined directly but can be measured quite accurately by an indirect approach. A fixed angular scale was mounted behind a pointer attached to the oscillator shaft. A strobe light, triggered by the same pulse which initiated the analyzer operation, was used to "stop" the pointer for a reading. In this manner, an angle corresponding to channel zero was read directly from the scale for various rotational frequencies of the oscillator rod. The accuracy of this reading was approximately $\pm$ 0.5 degrees. The reading obtained was a function of oscillator frequency since the pulse shape from the trigger coil was a function of the velocity of the permanent magnet attached to the oscillator rod. A curve showing the angular reading as a function of oscillator frequency is shown in Figure 12. The smooth curve that may be drawn through the data points indicates that the relative location of the pickup coil can be determined to approximately 0.2 degrees for any oscillator frequency.

The final step to obtain an absolute measurement of the phase lag between input and output was the calibration of the effect of the oscillator rod on the reactor as a function of angular position indicated by the pointer and fixed scale. The change in reactivity as a function of indicated angle was measured by determining the distance that a calibrated control rod of the reactor had to be moved to compensate for the angular motion of

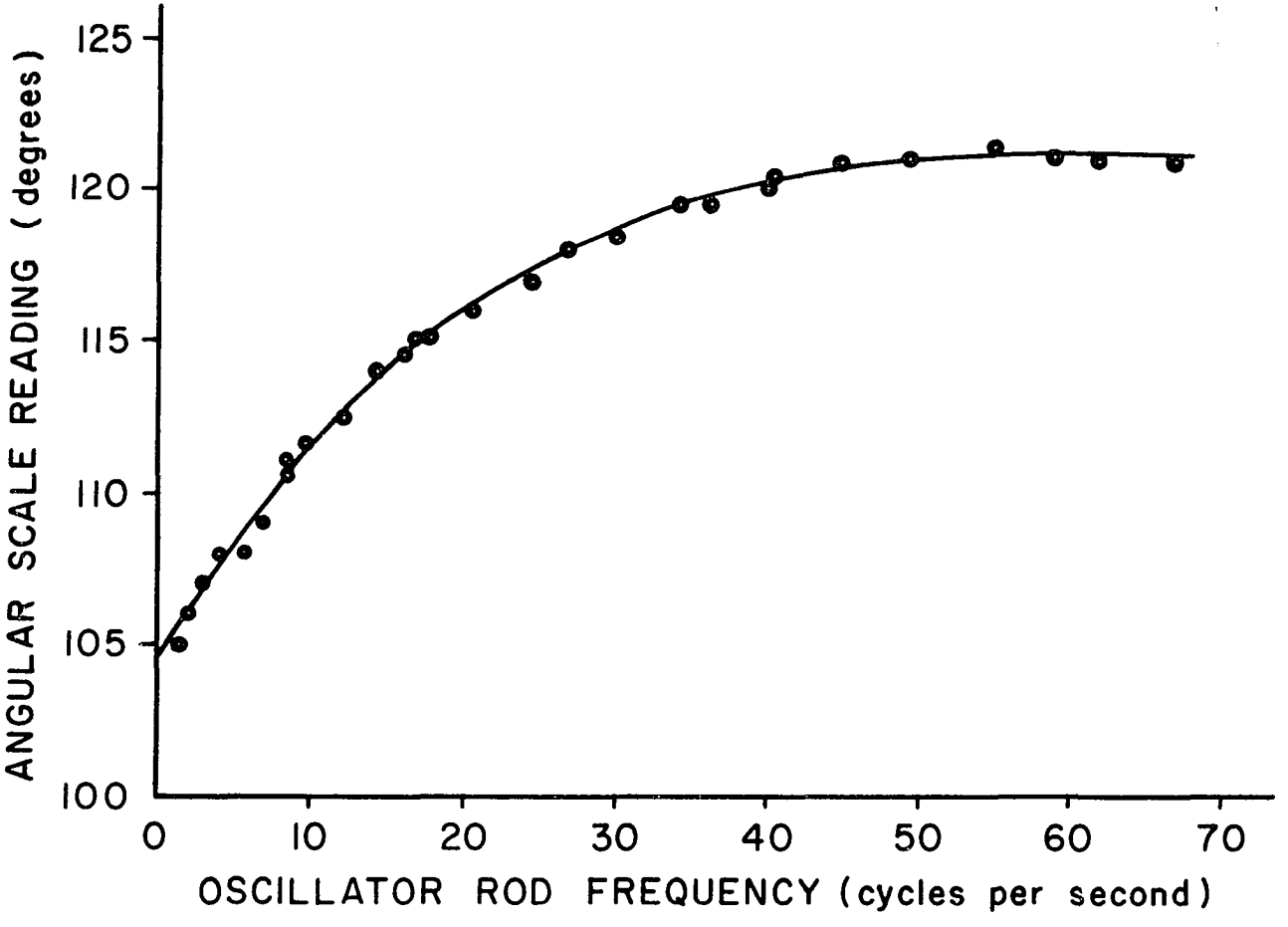

Reference Angle Reading as a Function of
Oscillator Rod Frequency

FIGURE 12

the oscillator rod. The control rod was calibrated with a technique previously developed by the author. [29] This calibration is very accurate in the range required for evaluation of the oscillator rod allowing the total worth of the oscillator to be determined to better than one per cent. The same type of least square fit program used for the output data was applied to the oscillator rod calibration data to determine phase angle of this calibration relative to the indicator reading. The calibration data together with the calculated curve is shown in Figure 13.

The absolute phase relation between input and output may now be determined since the output phase relative to the trigger pulse is known, the relation between trigger pulse and fixed scale is known as a function of the frequency and the phase relation between the input and the fixed scale is known. An accurate determination of the possible errors introduced in this complicated calibration procedure is difficult. The best reason for confidence in the numbers obtained lies in the fact that agreement between calculated and theoretical phase angle is very good. Since the absolute value of the phase angle was not one of the primary purposes of the research, an accurate error analysis has not been attempted. Primary interest was in the relative phase lag between measurements made at different spatial points which does not require

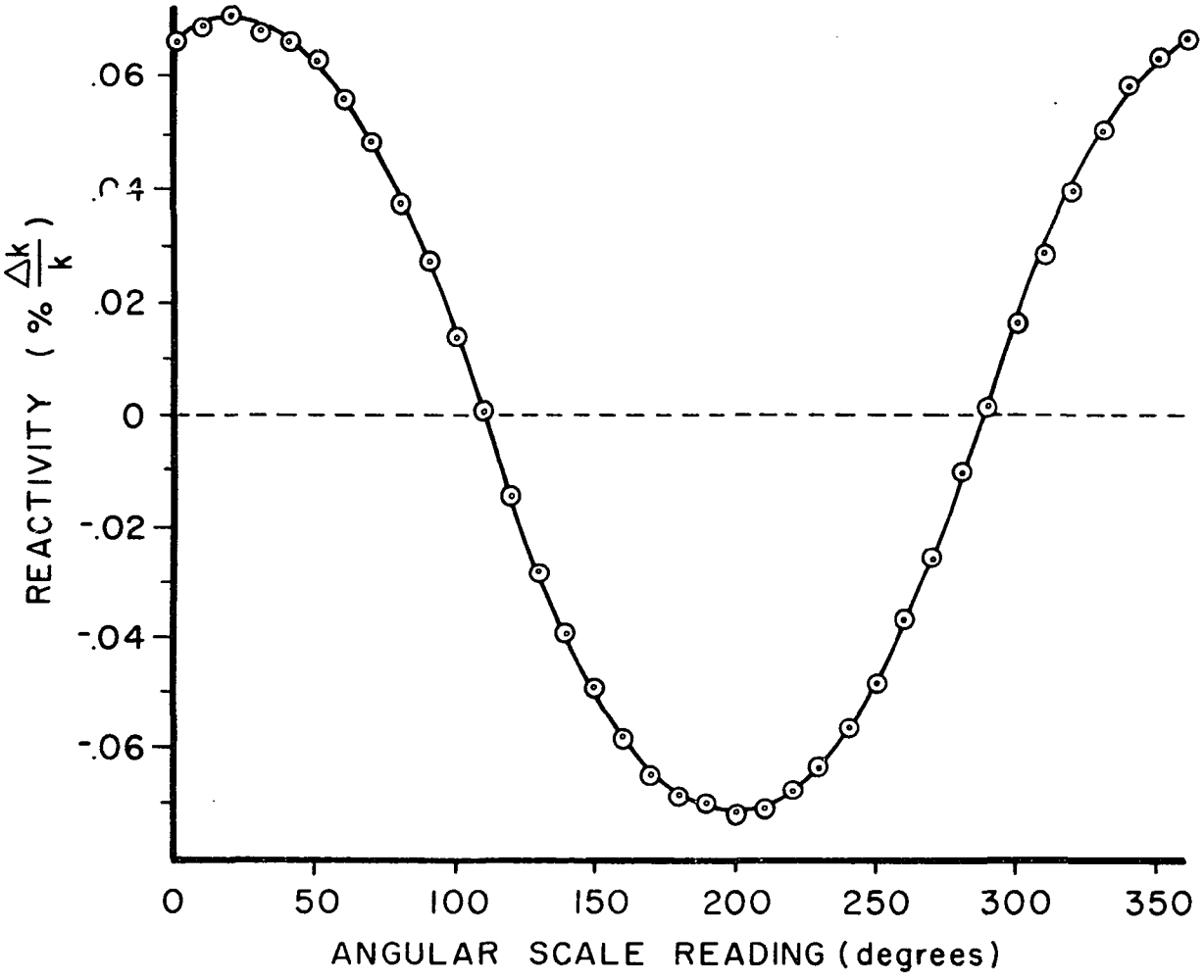

Oscillator Rod Calibration

FIGURE 13

knowledge of the absolute phase angle between input and output.

Figures 14 and 15 show the phase relationship between input and output as a function of oscillator frequency for two positions of the output detector. Sufficient data was obtained for such curves at eight other detector locations but the curves that result from these values are very similar to those in Figures 14 and 15 and have not been reproduced. A more suitable display of data is given later to show the relationship between phase lag and detector location.

Also shown on Figures 14 and 15 are curves relating the gain of the reactor to the oscillator frequency. The points plotted are determined from the definition

$$\text{Gain} = 20 \log \left| \frac{\Delta n}{n_o} \; \frac{\beta}{\Delta k} \right| . \qquad (51)$$

An experimental value for the neutron lifetime, ℓ^*, was obtained from the gain data as a least square fit to the approximate transfer function obtained from the linearized model of the point kinetic equations given previously. The ratio of $\gamma\beta$ to ℓ^* was taken as the parameter for this fit. Since $\gamma\beta$ is a known constant, the best value of ℓ^* was found to be

$$\ell^* = (6.0 \pm 0.08) \times 10^{-5} \text{ seconds.}$$

The value of ℓ^* was determined at each spatial point where the

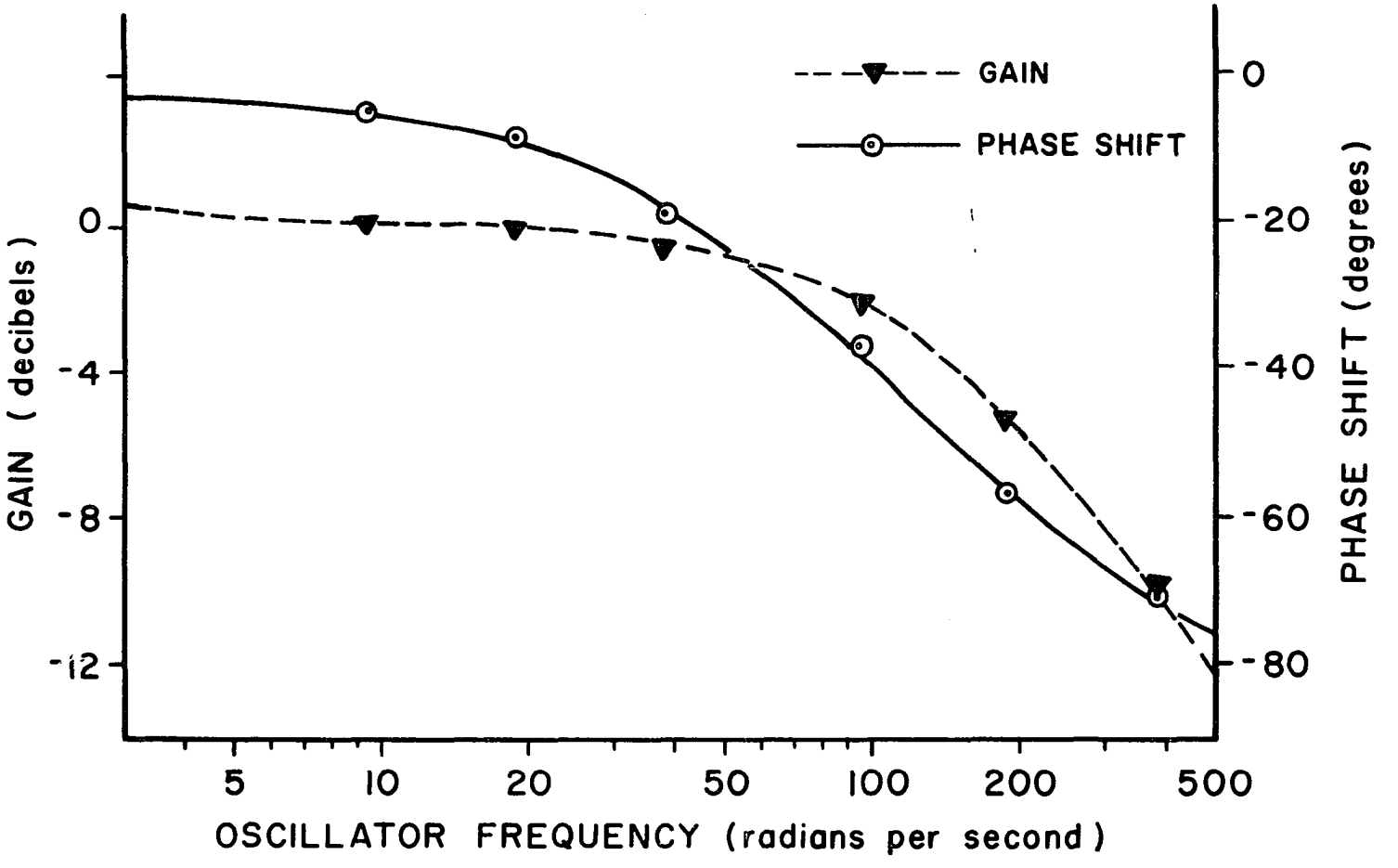

Reactor Gain and Phase Shift
15.2 cm. from Reactor Center

FIGURE 14

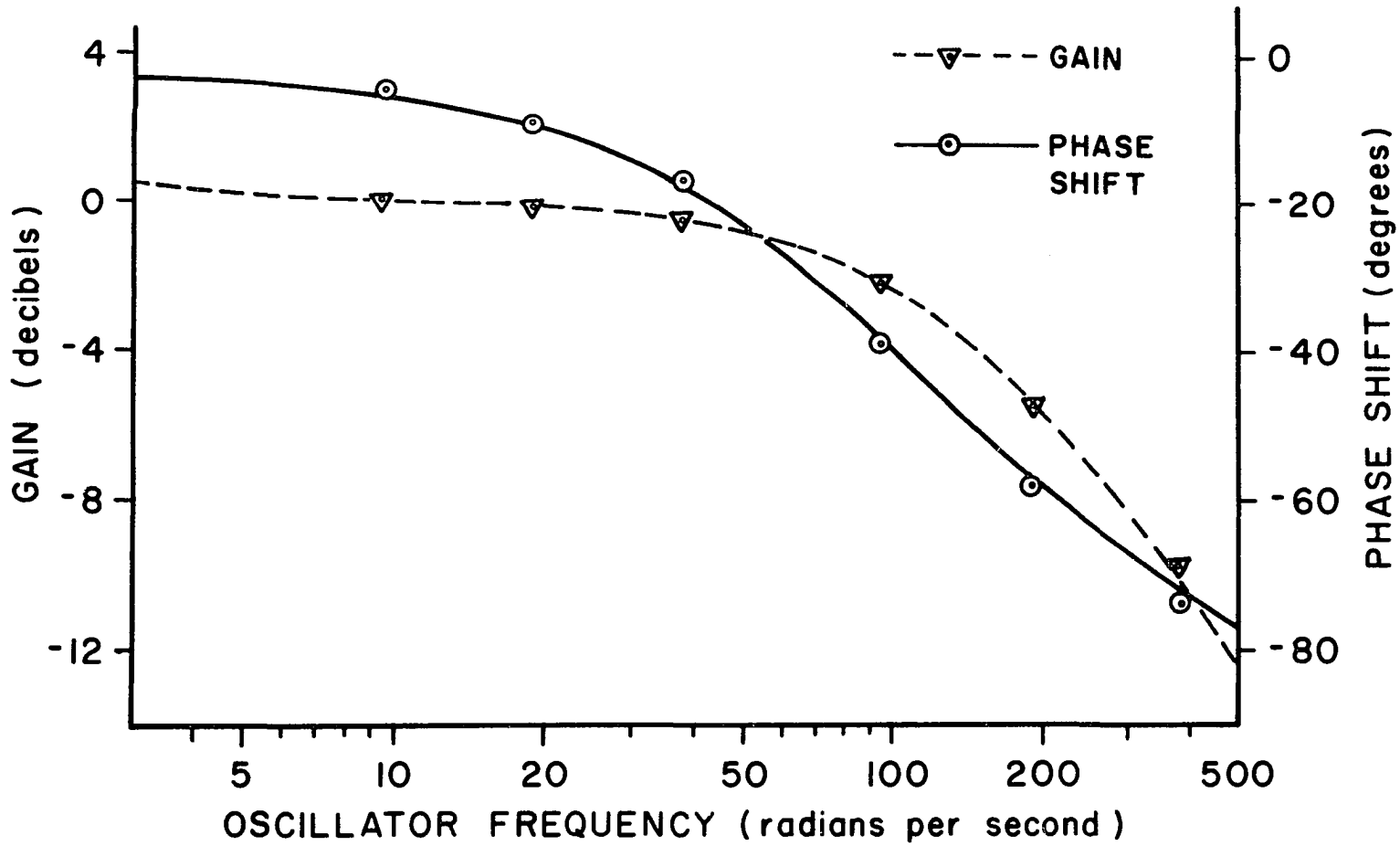

Reactor Gain and Phase Shift
43.2 cm. from Reactor Center

FIGURE 15

reactor frequency response was measured, but no significant variation of neutron lifetime with position could be observed. This observation was to be expected since the theoretical considerations predict a very small change in gain over the limited spatial range investigated. If it were possible to extend the experimental work to larger distances from the core the indicated value of the neutron lifetime should increase.

The value of ℓ^* as determined above was used to plot the theoretical curves of phase shift and gain in Figures 14 and 15 for comparison with the experimental points. The linearized model of the point kinetic equations was used for these curves.

While extending the experimental measurements to greater distances from the core would be desirable, it was not possible with the present experimental equipment. The limitation for the experimental work was determined by the sensitivity of the neutron detector used and the neutron flux available. Since it was essential to make point measurements of the neutron level, a small detector was required. Such a detector obviously has a small sensitive volume and consequently a low absolute sensitivity. The neutron flux available was limited by the maximum reactor power which, in turn, is fixed by The Atomic Energy Commission regulations governing operation of the reactor. The flux falls off sharply in the water surrounding the reactor core. The value of the flux relative to

the flux at the center of the reactor is shown in Figure 16. Both the thermal and the epithermal flux distributions are shown. These curves were obtained with the same detector used in the other experimental work. The distribtuion of the epithermal flux was measured by covering the detector with cadmium of sufficient thickness to absorb more than 99 per cent of the thermal neutrons. The thermal flux distribtuion was determined with the detector as normally used. The thermal readings were normalized to unity at the center of the reactor core and the ratio of the epithermal flux to thermal flux at the center of the core was calculated by means of the core coupling coefficient from two group diffusion theory. [3] [22] The group constants used in this calculation were calculated from the physical constants of the AGN-211 core material. [30] The coupling coefficient which determines the ratio of the epithermal to thermal flux at the center of the reactor is not dependent upon the geometry of the system but only upon the core materials. The epithermal to thermal flux ratio at points other than at the center is geometry dependent but may be determined from the ratio at the center and the flux distributions as a function of position in the region of interest. Values from these two curves were used to calculate the ratio of the slowing down density to the thermal diffusion density at the points where phase measurements

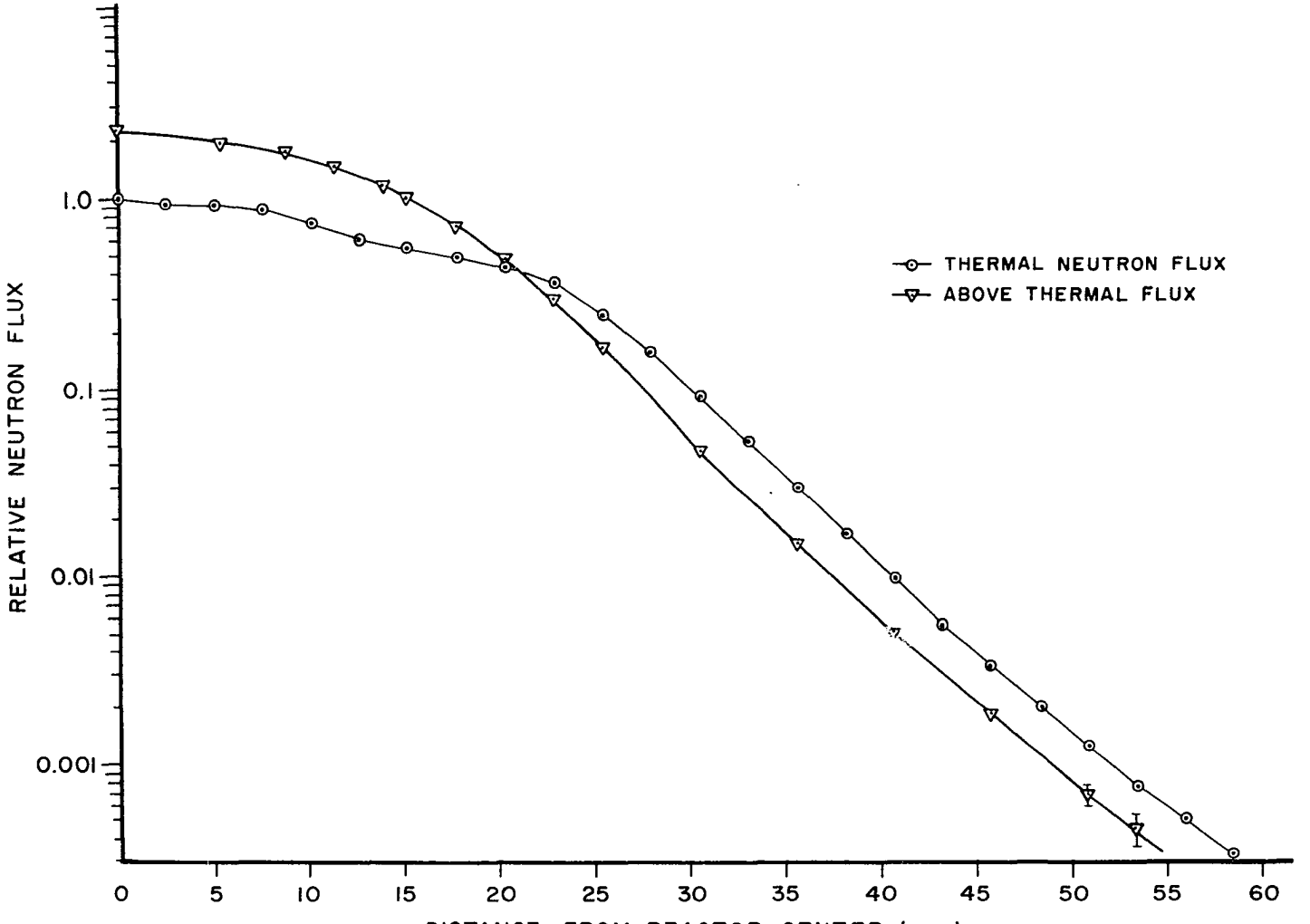

Neutron Flux Distribution as a Function of Position in Central Access Facility

FIGURE 16

were made. Since this latter ratio was required to predict the phase shift as a function of position, the experimental data for plotting these curves were obtained as accurately as possible. Sufficient counts were accumulated at each measurement point to insure a standard deviation of less than one-tenth per cent of the count with the exception of the last few points on the epithermal curve. The countrate observed with the cadmium covered detector at these distances was so low that extremely long counting times would have been required. Since the experimental measurements were not extended beyond 50 centimeters, these few points were not as accurately determined as those nearer the core. Standard deviation bars are shown on these points where the standard deviation exceeds the size of the point plotted. One other precaution taken to insure accurate flux distribution curves was to keep the oscillator rod running at 30 cps during these measurements. Any change in flux distribution induced by the rod would thus be the same as during the accumulation of other data. This effect should be very small since the oscillator rod was located several neutron mean free paths from the closest approach of the detector.

It is of interest to note that the slope of the curves in the water region surrounding the core is in agreement with that predicted by the one dimension two group diffusion equation for only a small distance

between 45 and 55 cm. The deviations outside this range are due to the complicated geometry of this reactor. The final results of the experimental work to verify the theoretical considerations discussed previously are displayed graphically in Figures 17 and 18. The graphs show the relation between phase lag and distance for the two frequencies where significant variations were observed. The data are plotted on an expanded scale so that variations will be more readily apparent. The data points shown are those determined from the relationship between input and output phase angle previously discussed in this chapter. The solid line in each graph is calculated by means of equation (42) developed in the theoretical section of this paper. Since equation (42) yields information concerning only phase change with position, the point at 15.2 cm. on each curve was taken as the phase lag predicted from the point kinetic equations for the particular frequency of interest. The phase shift calculated for each spatial point was then added to this value to obtain the total phase lag as a function of position. The dashed line on each graph is a line calculated by a least square fit of the experimental data to a straight line.

The data used to plot these two curves are presented in Tables 3 and 4. Also listed in these tables is the run number for determination of the output response. Consecutive run numbers indicate that the data

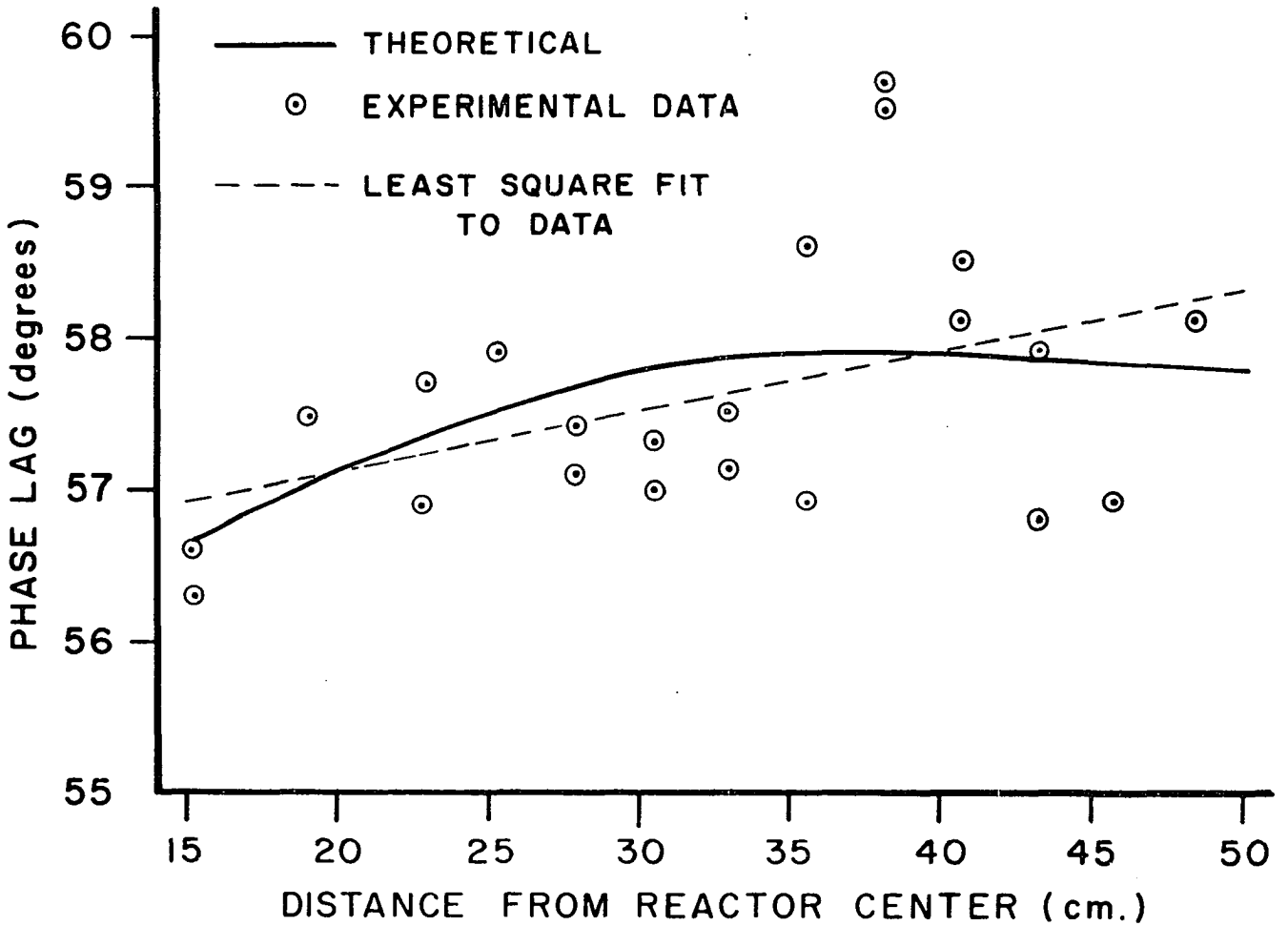

Phase Lag as a Function of Position at 30 cycles per second

FIGURE 17

TABLE 3

MEASURED AND CALCULATED PHASE LAG AT 30 CYCLES PER SECOND

Distance from Center	Run Number	Experimental Phase Lag Degrees	Calculated Phase Shift Degrees	Calculated Phase Lag Degrees
15.24	650 700	56.6 56.3	0.0	56.68
19.05	651	57.5	0.141	56.98
22.86	652 701	57.7 56.9	0.223	57.32
25.40	712	57.9	0.305	57.53
27.94	653 704	57.1 57.4	0.403	57.66
30.48	705 706	57.0 57.3	0.528	57.79
33.02	654 708	57.5 57.1	0.652	57.84
35.56	709 713	58.6 56.9	0.783	57.90
38.10	655 710	59.5 59.7	0.907	57.92
40.64	711 714	58.1 58.3	1.023	57.85
43.18	656 715	56.8 57.9	1.141	57.85
45.72	716	56.9	1.254	57.85
48.26	717	58.1	1.350	57.82
50.80			1.445	57.80

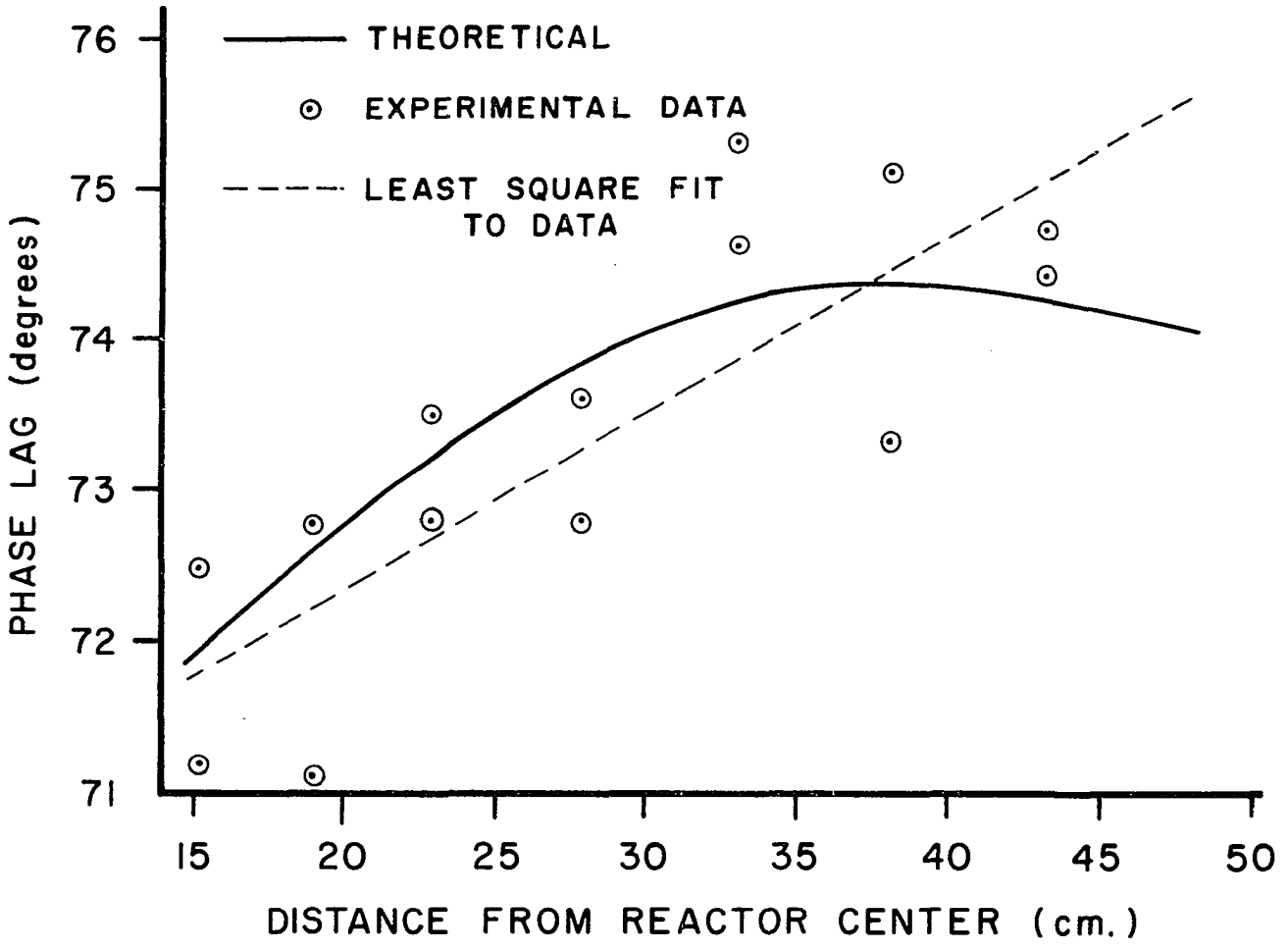

Phase Lag as a Function of Position at 60 cycles per second

FIGURE 18

TABLE 4

MEASURED AND CALCULATED PHASE LAG

AT 60 CYCLES PER SECOND

Distance from Center cm	Run Number	Experimental Phase Lag Degrees	Calculated Phase Shift Degrees	Calculated Phase Lag Degrees
15.24	323 389	71.2 72.5	0.0	71.92
19.05	324 601	72.8 71.1	0.296	72.53
22.86	325 386	73.5 72.8	0.446	73.19
27.94	326 385	73.6 72.8	0.805	73.86
33.02	327 384	74.6 75.3	1.305	74.24
38.10	328 383	73.3 75.1	1.814	74.40
43.18	329 382	74.4 74.7	2.282	74.25

points involved were obtained sequentially. This information is included to show that there is no apparent correlation of data with a particular experimental operation. A value of the variance may thus be determined considering all data accumulated at each frequency to be of equal weight. These run numbers also serve to identify the computer calculations and other operations necessary to reduce the data to the form given here.

CHAPTER VI

DISCUSSION OF RESULTS AND CONCLUSIONS

Experimental Errors

Two sources of error are predominant in the experimental results. They are the statistical nature of the accumulated data and the uncertainty of experimental parameters used in the reduction of the data.

Statistical Variations

For the counting of radiation from a radioactive source, Poisson statistics may be used. In counting neutrons from a nuclear reactor, however, the spread in the data is somewhat larger than that predicted by Poisson statistics if the counting time is short. The additional deviation is generally attributed to reactor noise which may be explained as resulting from chains of fission events originating from a single neutron. If a neutron initiated a chain which was perpetuated for some time, then it had a greater statistical weight than one which initiated a chain which terminated after only a few fissions. This effect decreases for higher operating powers since the number of such chains is larger and a better average is obtained. As the reactor power is increased or the counting time lengthened, the statistics approach

those predicted for a Poisson distribution.

For a Poisson distribution the standard deviation is equal to the square root of the number of counts obtained if this number is large. Thus,

$$s_e = \sqrt{N}$$

s_e = experimental standard deviation (52)

N = number of counts observed.

In the more general case, however,

$$s_c^2 = \frac{1}{n - 1} \sum_{i=1}^{n} (N_i - \overline{N})^2, \tag{53}$$

where

s_c^2 = calculated variance

n = the number of observations

N_i = number of counts observed in i^{th} observation

$\overline{N}$ = expected value of the observation

The value of s_c^2 was calculated by equation (53) in the data reduction program using the value predicted by equation (48) as $\overline{N}$. The value of s_c calculated from equation (53) in this manner was nearly the same as the value of s_e calculated from equation (52) using the mean value of the data as the value for N. This result would indicate that

the normal statistical variations involved in counting can account for the observed variations in the reduced data.

Since the mean value of the number of counts accumulated per channel was approximately 50,000, the standard deviation of 224 is 0.45 per cent of the observed number. The amplitude of the neutron variation was only 7 per cent of the mean value for the low frequency tests and dropped to 2.1 per cent for the sixty cycle per second tests. If the mean value is subtracted from the data points, then the deviation from the calculated variation ranges from 6.4 per cent to nearly 21 per cent of the amplitude of the variation. The scatter is shown graphically in Figure 11.

There are two ways of improving the accuracy of the experiment. The first would be to accumulate more counts in order to obtain a lower per cent standard deviation. Either the time required for the accumulation of data or the countrate would have to be increased with the result that other inaccuracies would be magnified as will be shown later. The other improvement could be made by increasing the total worth of the oscillator rod, thereby increasing the amplitude of the variation. This latter method cannot be used in the AGN-211 reactor since the available excess reactivity is quite low. The excess reactivity of the system limits the total worth of the oscillator rod as discussed in the previous chapter.

It appears, then, that the statistics are about what would be expected based on a Poisson distribution and that there is little chance of improving them. Runs in which the variance calculated from equation (53) was greater than 1.5 N were disregarded as having some other significant error. Less than 5 per cent of the data runs were discarded for this reason.

Experimental Parameters

The parameters required for the reduction of data are the values of Δt and ω used in equation (48). The method used to determine these parameters is discussed in the previous chapter.

Since most of the data used for this work was obtained with the oscillator driven by a synchronous motor, only the value of Δt is in question. Any variation of line frequency will appear as a change in Δt since Δt is measured relative to the line period.

A parameter study was made to find the effect of errors in the value of Δt. For this study the value of Δt used in the data reduction program was changed in steps of 0.1 per cent of the measured value of Δt for several steps each side of the measured value. This study showed that at 30 cycles per second a variation in the value of Δt of 0.1 per cent changed the computed value of the phase angle by 0.25 degrees. This effect was nearly the same for all frequencies--the

angular change being slightly greater at the higher frequencies and less at the lower frequencies. No change in calculated amplitude was observed for variations of Δt up to 0.4 per cent although the amplitude was calculated to four significant figures.

The effect of other parameters on the computed values was also checked experimentally. The reactor was operated at several power levels so that different countrates at a given position were utilized. The same number of counts was accumulated at each power level so that the statistical variations should have been the same. The computed variance was significantly larger at the lower power levels. The ratio of the amplitude of the variation to the mean value was also larger at lower countrates, but application of the correction factor given in Figure 8 brought the ratios into good agreement. No consistant variation of phase angle with countrate could be observed. All data runs except those at distances greater than 45 centimeters from the center were made at essentially the same average countrate. At the greater distances the flux was too low for the countrate normally used. The correction factors from Figure 8 were used to adjust all data for counting loss.

An attempt was made to determine the effect of slowly changing average power during the time required to accumulate data. No consistent variations were observed if the resulting calculations were

corrected to the average counting rate during the run.

It would appear that the most significant source of error in the calculated data can be attributed to inaccuracies in the value of Δt used in the computer calculations. The value of Δt was determined by measuring the pulse repetition rate from the time base generator as described in the previous chapter. The first pulser used as a time base generator was a General Radio Unit Pulser. Periodic calibration showed that the drift rate was often as high as 0.3 per cent per hour and was random in time. This pulser was replaced by a transistorized unit constructed for this experimental work. Calibration measurements were made at the beginning and end of each run. The observed drift did not exceed 0.4 per cent in any six hour period and appeared to be a function of temperature only. Since the Reactor Laboratory temperature did not cycle rapidly, the frequency drift was slow and uniform. The calibration procedure was accurate to only $\pm$ 0.1 per cent so that inaccuracies in the calculated phase of $\pm$ 0.25 degrees may have been introduced from this source.

Observed Variance of Data

The most significant results of the study to investigate the measured phase lag as a function of distance between the reactor and the detector are shown graphically in Figure 17 and Figure 18. The experimental

data on these two curves show considerable dispersion. A least square fit to a straight line, represented by the dashed line in each graph, was calculated to show the trend in the data. The calculated variance of the data to this line was 0.59 for both the 30 cycle and 60 cycle per second data, which represents a dispersion of 0.77 degrees.

The solid curve calculated from the equations of Chapter III represents a better fit to the data. The variance from the calculated curve is 0.53 for the 60 cycle per second data shown in Figure 18 and 0.55 for the 30 cycle per second data shown in Figure 17. Since there exists a strong possibility of a consistent error in obtaining the absolute phase lag by the method outlined in the previous chapter the effect of moving all data points was investigated. This movement will not change the least square fit to a straight line, but does change the variance computed from the theoretical curve. In both cases the variance could be minimized by adding 0.1 degree to all data. The values of the data points obtained in this manner may be considered the best fit of the data to the theory.

The variance between the 60 cycle per second data and the best straight line is 11.4 per cent greater than the variance between the data and the best fit to the theory. The variance between the 30 cycle per

second data and the best straight line is 7.9 per cent greater than the variance between the data and the best fit to the theory.

No trend could be observed in the ratio of the amplitude of the variation to the mean neutron level with position. However, in the range of these investigations, any trend, if existant, would be very small.

Conclusions

The experimental verification of the phase shift predicted in a diffusion medium by equation (42) indicates that the theoretical model developed in Chapter III is a valid representation of the system. Application of the theory to media other than water should also be verified experimentally. Unless experimental verification is made to evaluate the approximations incorporated in equation (42), the more general expression, equation (34), should be used to predict the phase as a function of position, and equation (46) should be used to predict the attenuation.

Water has a unique property among the common materials used for neutron reflection and moderation. The value of Σ_a / D_{th} is larger than the value of $1/\tau$. The significance of this may be seen from an examination of equations (22) and (23) relating the spatial distribution of the flux to position for fast and thermal neutrons. It can be seen

that for water the first term in equation (23) will decrease more rapidly than the second so that at large distances from the core the second term predominates. For large distances then

$$\phi_1(x) = \phi_{10}\, e^{-\left[\frac{1}{\tau}\right]^{\frac{1}{2}}(x - x_0)} \tag{54}$$

$$\phi_2(x) \cong F\, \phi_{10}\, e^{-\left[\frac{1}{\tau}\right]^{\frac{1}{2}}(x - x_0)}, \tag{55}$$

and the ratio of $\phi_2(x)$ to $\phi_1(x)$ becomes a constant, F. This condition may be observed in Figure 16. From the expression for F given by equation (24) and the material constants for water stated previously, F = 2.5. The experimental value of F, determined from the data of Figure 16, is 2.0 in the range where the slopes are in agreement with equations (54) and (55). This discrepancy would indicate that the two group, one dimension diffusion equation used does not accurately describe the system studied. It is adequate, however, to allow prediction of a limiting value for the phase shift in water. This limiting action should not be the case in other moderator materials such as graphite, beryllium or heavy water. For these materials, the phase shift should approach a constant slope, rather than a constant value, since the fast group flux decreases more rapidly with position than the thermal group.

The experimental results verify that the semi-empirical equations developed in Chapter III are a valid model for the interpretation of frequency response measurements. Equations (45) and (46) may be used to calculate the frequency response of the reactor core when the measurements are made some distance from the core itself. Parameters of the reactor core may then be determined in the usual manner from the kinetic equations.

LIST OF REFERENCES

1. G. Goertzel, "Reactor Dynamics," The Reactor Handbook, Vo. 1, AECD-3645, (1955).
2. M. A. Schultz, Control of Nuclear Reactors and Power Plants, 2nd Edition, McGraw-Hill Book Company, Inc., (1961).
3. R. V. Meghreblian and D. K. Holmes, Reactor Analysis, McGraw-Hill Book Company, Inc., (1960).
4. A. M. Weinberg and E. P. Wigner, The Physical Theory of Neutron Chain Reactors, The University of Chicago Press, (1958).
5. G. M. Wing, An Introduction to Transport Theory, John Wiley and Sons, Inc., (1962).
6. F. J. Henry, "The Application of Reactor Kinetics to the Analysis of Experiment," Nuclear Sci. and Eng., 3, 52-70, (1958).
7. S. Kaplan, "The Property of Finality and the Analysis of Problems in Reactor Space-Time Kinetics by Various Modal Expansions," Nuclear Sci. and Eng., 9, 357-361, (1961).
8. H. B. Smets, "The Effect of Burnable Fission Products in Power Reactor Kinetics," Nuclear Sci. and Eng., 11, 133-141, (1961).
9. D. E. Dougherty and C. N. Shen, "The Space-Time Neutron Kinetics Equations Obtained by the Semidirect Variational Method," Nuclear Sci. and Eng., 13, 141-148, (1962).

10. C. E. Cohn, "Reflected Reactor Kinetics, "Nuclear Sci. and Eng., 13, 12-17, (1962).

11. H. L. Garabedian and C. B. Leffert, "A Time Dependent Analysis of Spatial Flux Distributions, "Nuclear Sci. and Eng., 6, 26, (1959).

12. A. Foderaro and H. L. Garabedian, "Two Group Reactor Kinetics," Nuclear Sci. and Eng., 14, 22-29, (1962).

13. Proceedings of the Conference on Transfer Function Measurement and Reactor Stability Analysis, ANL-6205, (1960).

14. R. M. Kiehn, "Frequency Analysis for LAMPRE," K-1-2369 (Los Alamos Interdivision Memo), (1956).

15. J. D. Balcomb, H. B. Demuth, and E. P. Gyftopoulos, "A Cross-correlation Method for Measuring the Impulse Response of Reactor Systems, "Nuclear Sci. and Eng., 11, 159-166, (1961).

16. V. Rajagopal, "Determination of Reactor Transfer Functions by Statistical Correlation Methods," Nuclear Sci. and Eng., 12, 218-224, (1962).

17. A. R. Boynton and R. E. Uhrig, "Evaluation of Two-Region-Reactor Parameters by Random Noise Measurements, "Nuclear Sci. and Eng., 18, 220-229, (1964).

18. M. N. Moore, "The Determination of Reactor Transfer Functions From Measurements at Steady Operation," Nuclear Sci. and Eng., 3, 387-394, (1958).

19. C. W. Griffin and R. L. Randall, "At Power, Low Frequency, Reactor-Power-Spectrum Measurements and Comparison with Oscillation Measurements, " Nuclear Sci. and Eng., 15, 131-138, (1963).

20. Proceedings of the Brookhaven Conference on Neutron Thermalization, Vols, I, II, III, and IV, BNL 719, (1962).

21. K. H. Beckurts, "Transient Effects in Space, Time and Energy," BNL 719, Vol. III, RE-1 - RE-62, (1962).

22. R. L. Murray, Nuclear Reactor Physics , Prentice-Hall, Inc., (1957).

23. R. B. Perez and R. E. Uhrig, "Propagation of Neutron Waves in Moderating Media," Nuclear Sci. and Eng., 17, 99-100, (1963).

24. R. E. Uhrig, "Oscillatory Techniques in a Subcritical Assembly," Proceedings of the University Subcritical Assemblies Conference, TID-7619, 161-182, (1961) .

25. E. Garelis and J. L. Russell, "Theory of Pulsed Neutron Source Measurements," Nuclear Sci. and Eng., 16 , 263-270, (1963).

26. E. Garelis, "Theory of Pulsing Techniques, " Nuclear Sci. and Eng., 18 , 242-245, (1964).

27. G. R. Keepin, T. F. Wimett, R. K. Zeigler, "Delayed Neutrons from Fissionable Isotopes of Uranium, Plutonium and Thorium," The Phys. Rev. 107, 1044-1049, (1957).

28. D. J. Hughs, R. B. Schwartz, "Neutron Cross Sections," BNL 325, 331-336, (1958).

29. A. E. Wilson, "Reactor Control Rod Calibration," Proc. American Nuclear Society, 3, No. 2, (1960).

30. Aerojet General Nucleonics, "AGN-211 Reactor Manual," AGN-3009, (1958).

APPENDIX A

DERIVATION OF THE REACTOR KINETIC EQUATIONS

The transport of neutrons in a medium in which the probability of absorption is small compared to the probability of scattering may be described by neutron diffusion equations. In the simplest form

$$\frac{\partial n}{\partial t} = D\nabla^2 \phi + \nu \Sigma_f \phi - \Sigma_a \phi \qquad \text{(A-1)}$$

where:

n = the neutron density

D = the diffusion coefficient of the medium

ϕ = the neutron flux

Σ_a = macroscopic absorption cross section of the medium

Σ_f = macroscopic fission cross section of the medium

ν = average number of neutrons produced per fission.

This equation is applicable only if all neutrons have the same energy, if the medium is homogeneous and if there are no neutron sources other than fission neutrons. If these conditions are met, a solution may be obtained by assuming that ϕ is a product of a function of space and a function of time. The definition of neutron flux, $\phi = nv$, where v is the neutron

velocity may be used to obtain

$$\frac{1}{v} \frac{\partial \phi}{\partial t} = D\nabla^2 \phi - \Sigma_a \phi + \nu\Sigma_f\phi. \qquad \text{(A-2)}$$

The equation (A-2) has been used extensively to develop a set of reactor kinetic equations to describe the time dependent behavior of nuclear reactors. The development is included here to show what further approximations and assumptions must be made to obtain the kinetic equations.

Since the primary interest is now in the time dependent behavior of the reactor, the source term in equation (A-2), $\nu\Sigma_f\phi$, is not an adequate representation as it would imply that all neutrons are produced at the time of fission. Actually, a small fraction of the neutrons are delayed--being essentially trapped in radioactive nuclides and released only at the time of decay of the nuclide--so that the neutron source should be split into a prompt term, S_p, and a delayed term, S_d, or

$$\frac{\partial n}{\partial t} = D\nabla^2 \phi - \Sigma_a \phi + S_p + S_d. \qquad \text{(A-3)}$$

The first assumption that must be made is that the spatial distribution of the neutron flux does not change with time so that the spatial solution to the steady state problem may be used in the non-steady state case. For the steady state case

$$\nabla^2 \phi + B^2 \phi = 0 \qquad \text{(A-4)}$$

B^2 is the reactor buckling and includes all of the constants of equation

(A-2). Here it is permissible to lump the prompt and delayed source terms together since steady state is assumed.

Care must be taken in the use of the diffusion equation since all of the neutrons are not of the same energy. The effect of slowing down from fission neutron energies to the energy at which the neutrons are absorbed may be incorporated in the effective multiplication factor, k_e, for a thermal reactor.

$$k_e = \eta \, f \, \varepsilon \, p \, F_t \, F_f \qquad \text{(A-5)}$$

where:

η = the number of fast neutrons produced (both prompt and delayed) per thermal neutron absorbed in the fuel

f = the thermal utilization

ε = the fast fission factor

p = the resonance escape probability

F_t = the thermal non leakage probability

F_f = the fast non leakage probability.

It can be shown that for a bare, homogeneous reactor which is many neutron mean free paths across

$$F_t = \frac{1}{B^2 L^2 + 1} \qquad \text{(A-6)}$$

$$L^2 = \frac{D}{\Sigma_a} \qquad \text{(A-7)}$$

The neutron lifetime, ℓ, may now be defined as

$$\ell = \frac{\text{the number of neutrons present at steady state}}{\text{the rate of supply of neutrons}} .$$

The rate at which neutrons are supplied per cubic centimeter to the system in steady state would be simply the source term in equation (A-2) if the neutrons were absorbed without energy loss. For a thermal reactor, however, not all of the fast neutrons produced by fission reach thermal energies so that the rate of supply of neutrons must be modified by the probabilities listed under equation (A-5). With this modification

$$\ell = \frac{n}{\phi \Sigma_f \nu F_f p \varepsilon} . \qquad \text{(A-8)}$$

For non steady state, the rate of supply is dependent upon the neutron concentration in the previous generation, $\frac{n}{k_e}$, and the lifetime, ℓ^*, is

$$\ell^* = \frac{n \eta f \varepsilon p F_f F_t}{\phi \Sigma_f \nu F_f p \varepsilon} = \frac{n F_t}{\Sigma_a \phi} \qquad \text{(A-9)}$$

since

$$\nu \Sigma_f = \eta \Sigma_a f \text{ and } \ell^* = k_e . \qquad \text{(A-10)}$$

The combination of equations (A-3), (A-4) and (A-6) yields

$$\frac{\partial n}{\partial t} = - \frac{\phi \Sigma_a}{F_t} + S_p + S_d$$

but the first term on the right may be simplified by using the value of ϕ from equation (A-9) and since the spatial dependence has been removed by the use of equation (A-4), the partial derivative of n with respect to t may be replaced by the total derivative.

$$\frac{dn}{dt} = - \frac{n}{\ell^*} + S_p + S_d . \qquad \text{(A-11)}$$

If a fraction, β, of the neutrons produced by fission are delayed, then only a portion, $1 - \beta$, of the neutron production rate used in equation (A-9) comprises the prompt source, S_p.

$$S_p = \phi \Sigma_a \eta \, f \, \varepsilon \, p \, F_f' \, (1 - \beta) \qquad \text{(A-12)}$$

where F_f' may differ from the average value, F_f, if the energy of the prompt neutrons is different from the average neutron energy at the time of production. Using the previous definitions

$$S_p = \frac{k_e}{\ell^*} \, n \, (1 - \beta) \, \frac{F_f'}{F_f} . \qquad \text{(A-13)}$$

The rate at which delayed neutrons are produced is equal to the rate of decay of the delayed neutron precursor nuclides. The delayed source term, S_d, is the rate at which these delayed neutrons reach thermal energies so that for the i-th group

$$S_{di} = \lambda_i \, c_i \, p_i \, F_{fi} \qquad \text{(A-14)}$$

where:

c_i = the concentration of the i-th precursor group

λ_i = the decay constant of the i-th precursor group

p_i = the resonance escape probability of the i-th group

F_{fi} = the fast non leakage probability of the i-th group.

Since the energy at which the delayed neutrons are produced is above the resonance capture region, a good approximation is that $p_i = p$ for all delayed groups because all neutrons must slow down through the same resonance region. F_{fi} may be quite different from F_f for much of the fast leakage occurs at the highest neutron energies. A weighted average of F_f' and the F_{fi} will be used for F_f.

$$F_f = F_f'(1 - \beta) + \sum_{i=1}^{6} F_{fi}\,\beta_i \qquad \text{(A-15)}$$

where β_i is the fraction of fission neutrons which are delayed in the i-th group. The delayed neutron effectiveness is now defined as

$$\gamma_i = \frac{F_{fi}}{F_f} \qquad \text{(A-16)}$$

Also

$$\gamma\,\beta = \sum_{i=1}^{6} \gamma_i\,\beta_i\,. \qquad \text{(A-17)}$$

Then, from (A-15)

$$F_f'(1 - \beta) = F_f(1 - \gamma\,\beta) \qquad \text{(A-18)}$$

The source terms may now be written as

$$S_p = \frac{k_e}{\ell^*} \, n \, (1 - \gamma\beta) \tag{A-19}$$

and

$$S_{di} = \lambda_i \, c_i \, p \, \gamma_i \, F_f \, . \tag{A-20}$$

The effective precursor concentration, C_i, may be defined as

$$C_i = c_i \, p \, F_f \, . \tag{A-21}$$

Substituting this into equation (A-20) and summing S_{di} over all i to obtain S_d

$$S_d = \sum_{i=1}^{6} \gamma_i \, \lambda_i \, C_i \, . \tag{A-22}$$

Substituting equations (A-22) and (A-19) into (A-11) yields

$$\frac{dn}{dt} = - \frac{n}{\ell^*} + \frac{k_e}{\ell^*} \, n \, (1 - \gamma \beta) + \sum_{i=1}^{6} \gamma_i \, \lambda_i \, C_i$$

$$= \frac{(k_e - 1) - \gamma \beta k_e}{\ell^*} \, n + \sum_{i=1}^{6} \gamma_i \, \lambda_i \, C_i \, . \tag{A-23}$$

Six more relationships are required to evaluate the C_i in (A-23). They may be obtained by means of a material balance on each of the six precursor groups. The rate of production of the c_i nuclides is just β_i times the neutron production rate from fission and the loss

rate is the decay rate of the c_i nuclides.

$$\frac{dc_i}{dt} = \nu\Sigma_f \varepsilon \phi \beta_i - \lambda_i c_i \tag{A-24}$$

but $\nu\Sigma_f = f\eta \Sigma_a$ and $c_i = \frac{C_i}{p F_f}$ so that

$$\frac{dC_i}{dt} = \eta f p \varepsilon \Sigma_a F_f \phi \beta_i - \lambda_i C_i \tag{A-25}$$

and from the definitions of k_e and ℓ^*

$$\frac{dC_i}{dt} = \frac{k_e \beta_i}{\ell^*} n - \lambda_i C_i \ . \tag{A-26}$$

For steady state operation, k_e must be equal to unity so that deviations from steady state can be most easily described by the deviation of k_e from one. Let

$$\Delta k_e = k_e - 1 . \tag{A-27}$$

The set of seven simultaneous differential equations referred to as the nuclear reactor kinetic equations are then

$$\frac{dn}{dt} = \frac{\Delta k_e - \gamma \beta k_e}{\ell^*} n + \sum_{i=1}^{6} \gamma_i \lambda_i C_i \tag{A-28}$$

$$\frac{dC_i}{dt} = \frac{k_e \beta_i}{\ell^*} n - \lambda_i C_i ; \quad i = 1 \text{ to } 6. \qquad \text{(A-29)}$$

The conditions that should be satisfied for application of the kinetic equations are those assumed for the derivation of the diffusion equation plus the approximations made subsequently to obtain the kinetic equations. One condition, that of monoenergetic neutrons, may be relaxed since the effect of slowing down from fission energies to thermal energies has been accounted for to some extent. It has been found experimentally that the kinetic equations are a valid description of many systems where these conditions are not satisfied. The equations have found widespread use in studies of the stability and transient behavior of most types of nuclear reactors.

APPENDIX B

LINEARIZATION AND TRANSFORMATION OF THE REACTOR KINETIC EQUATIONS

The kinetic equations developed in Appendix A may be linearized and transformed to obtain a transfer function which is useful in frequency response studies of a nuclear reactor. The linearization may be accomplished by assuming that:

$$n = n_0 + \Delta n \tag{B-1}$$

$$C_i = C_{i0} + \Delta C_i \tag{B-2}$$

$$k_e = 1 + \Delta k_e \tag{B-3}$$

where Δn, ΔC_i and Δk_e are small variations about the respective steady state values, n_0, C_{i0} and unity.

If these values are substituted into equations (A-28) and (A-29) and all terms involving products of the variations are dropped as negligibly small compared to the other terms then

$$\frac{dn_0}{dt} = \frac{\Delta k_e - \gamma \beta k_e}{\ell^*} n_0 - \frac{\gamma \beta}{\ell^*} \Delta n + \sum_{i=1}^{6} \gamma_i \lambda_i C_{i0} + \sum_{i=1}^{6} \gamma_i \lambda_i \Delta C_i \tag{B-4}$$

$$\frac{dC_{i0}}{dt} + \frac{d\Delta C_i}{dt} = \frac{\beta_i k_e}{\ell^*} n_0 + \frac{\beta_i}{\ell^*} \Delta n$$

$$- \lambda_i (C_{i0} - \Delta C_i). \qquad \text{(B-5)}$$

Equations (A-28) and (A-29) are assumed valid under any conditions so that

$$\frac{dn_0}{dt} = \frac{\Delta k_e - \gamma \beta k_e}{\ell^*} n_0 + \sum_{i=1}^{6} \gamma_i \lambda_i C_{i0} \qquad \text{(B-6)}$$

$$\frac{dC_{i0}}{dt} = \frac{\beta_i k_e}{\ell^*} n_0 - \lambda_i C_{i0}. \qquad \text{(B-7)}$$

Subtracting (B-6) from (B-4) and (B-7) from (B-5)

$$\frac{d\Delta n}{dt} = \frac{\Delta k_e}{\ell^*} n_0 - \frac{\gamma \beta}{\ell^*} \Delta n + \sum_{i=1}^{6} \gamma_i \lambda_i \Delta C_i \qquad \text{(B-8)}$$

$$\frac{d\Delta C_i}{dt} = \frac{\beta_i}{\ell^*} \Delta n - \lambda_i \Delta C_i. \qquad \text{(B-9)}$$

Equation (B-8) may be simplified by substituting the value of $\lambda_i \Delta C_i$ from equation (B-9) and recalling that

$$\sum_{i=1}^{6} \gamma_i \beta_i = \gamma \beta. \qquad \text{(A-17)}$$

The following set of linearized equations is then obtained

$$\frac{d\Delta n}{dt} = \frac{\Delta k_e}{\ell^*} n_0 - \sum_{i=1}^{6} \gamma_i \frac{d\Delta C_i}{dt} \qquad \text{(B-10)}$$

$$\frac{d\Delta C_i}{dt} = \frac{\beta_i}{\ell^*} \Delta n - \lambda_i \Delta C_i, \quad i = 1 \text{ to } 6. \qquad \text{(B-9)}$$

These equations may now be transformed assuming zero initial conditions to obtain

$$s\ \Delta n(s) = \frac{n_0}{\ell^*} \Delta k_e(s) - s \sum_{i=1}^{6} \gamma_i \Delta C_i(s) \qquad \text{(B-11)}$$

$$s\ \Delta C_i(s) = \frac{\beta_i}{\ell^*} \Delta n(s) - \lambda_i \Delta C_i(s), \quad i = 1 \text{ to } 6. \qquad \text{(B-12)}$$

Equations (B-11) and (B-12) may be reduced to a single equation

$$\frac{\Delta n(s)}{\Delta k_e(s)} = \frac{n_0}{\ell^*} \frac{1}{s\left[1 + \sum_{i=1}^{6} \frac{\beta_i \gamma_i}{\ell^*(s + \lambda_i)}\right]} . \qquad \text{(B-13)}$$

By expanding the summation in equation (B-13) and multiplying both the numerator and denominator by the product

$$(s + \lambda_1)(s + \lambda_2)(s + \lambda_3)(s + \lambda_4)(s + \lambda_5)(s + \lambda_6)$$

the equation may be reduced to form

$$\frac{\Delta n(s)}{\Delta k_e(s)} = \frac{n_0}{\ell^*} \frac{\prod_{i=1}^{6} (s + \lambda_i)}{\prod_{i=1}^{6} (s + r_i)} \qquad \text{(B-14)}$$

where the r_i are the roots of the denominator. These roots may be found for any system if the values of β_i, γ_i, λ_i, and ℓ^* are known. Using the values of λ_i and β_i determined by Keepin, Wimett and Zeigler [27] for uranium-235 fuel it can be shown that for values of ℓ^* less than 10^{-4} seconds: [2]

$$\frac{\Delta n(s)}{\Delta k_e(s)} = \frac{n_0}{\ell^*} \frac{(s+3.01)(s+1.14)(s+0.301)(s+0.111)(s+0.0305)(s+0.0124)}{s(s+\frac{\gamma\beta}{\ell^*})(s+2.40)(s+1.020)(s+0.159)(s+0.0681)(s+0.0143)} \qquad \text{(B-15)}$$

is a very good approximation.

To obtain a function to describe the frequency response of the reactor it is necessary to replace s by $j\omega$ in the above expression. ω is the system frequency in radians per second and j is the square root of -1. The problem of rationalizing the resulting expression to obtain the gain and phase shift may best be handled graphically. For frequencies greater than 10 radians per second, however, only the shortest system time constant is important and the following approximation may be used

$$\frac{\Delta n(j\omega)}{\Delta k_e(j\omega)} = \frac{n_0}{\ell^*} \frac{1}{j\omega + \frac{\gamma\beta}{\ell^*}} \; . \qquad \text{(B-16)}$$

This approximation improves with increasing frequency.

In experimental work in reactor kinetics it is more convenient to work with a normalized form of equation (B-16).

$$\frac{\frac{\Delta n(j\omega)}{n_0}}{\frac{\Delta k_e\,(j\omega)}{\gamma\beta}} = \frac{1}{j\omega\frac{\ell^*}{\gamma\beta} + 1} \tag{B-17}$$

The ratio of Δn to n_0 allows the use of a detector system in which the absolute sensitivity is not known and permits comparison of measurements made at different steady state levels. Using the ratio of Δk_e to $\gamma\beta$ as an input function allows comparison between reactors which have different delayed neutron effectiveness factors or different nuclear fuels.

Let

$$\frac{\frac{\Delta n(j\omega)}{n_0}}{\frac{\Delta k_e(j\omega)}{\gamma\beta}} = G(j\omega) \tag{B-18}$$

and

$$\frac{\ell^*}{\gamma\beta} = T \tag{B-19}$$

Then

$$G(j\omega) = \frac{1}{j\omega T + 1} = \frac{1 - j\omega T}{1 + \omega^2 T^2} \tag{B-20}$$

and the gain and phase shift may be calculated in the usual manner as

$$\text{Gain} = 10 \log \frac{1}{1 + \omega^2 T^2} . \tag{B-21}$$

$$\text{Phase shift} = \tan^{-1}(-\omega T) . \qquad \text{(B-22)}$$

Equations (B-21) and (B-22), while based on several approximations, will be used for comparison purposes in analyzing the experimental data.

APPENDIC C

NOMENCLATURE

A	Average value of the output signal from data reduction program
A_m	Relative fraction of the output reaching the m-th spatial point by thermal diffusion
B	Constant in the data reduction program
B^2	Reactor bucking constant
B_m	Relative fraction of the output reaching the m-th spatial point by fast diffusion and slowing down
C	Constant in the data reduction program
c_i	Delayed neutron precursor concentration for the i-th group
C_i	Effective delayed neutron precursor concentration for the i-th group
C_m	Relative amplitude of the output signal at the m-th spatial point
D	Diffusion coefficient
D_1	High energy group diffusion coefficient
D_2	Low energy group diffusion coefficient
D_{th}	Thermal energy group diffusion coefficient
f	Oscillator frequency, cycles per second, equation (48) only

f	Thermal utilization
F	A constant in the solution to the two group steady state diffusion equations
F_f	Fast nonleakage probability
F_t	Thermal nonleakage probability
$G(s)$	Reactor transfer function
i	Subscript denoting precursor group for delayed neutrons
j	Subscript denoting spatial position
k_e	Effective multiplication constant
ℓ^*	Effective neutron lifetime
m	Subscript denoting spatial position
n	Neutron concentration
n_0	Neutron concentration at steady state
p	Resonance escape probability
s	Complex domain
s_c^2	Calculated variance of experimental data to computer fit
S_d	Delayed neutron source
s_e	Standard deviation of a Poisson distribution
S_p	Prompt neutron source
t	Time
T	Shortest system time constant
Δt	Time interval for data accumulation
v	Neutron velocity

x	Position
y_n	Computed value of the neutron output at the n-th time interval
a_j	Phase shift between core response and response measured at the j-th spatial point
β	Fraction of the fission neutrons which are delayed
γ	Effectiveness of delayed neutrons
Δ	Variation
ε	Fast Fission Factor
$\varepsilon(x,t)$	Time dependent portion of the solution to the diffusion equation
η	Number of neutrons produced per neutron absorbed in reactor fuel
θ	Phase shift between output and input
λ_i	Decay constant of the i-th delayed group
ν	Number of neutrons produced per fission
Σ_a	Macroscopic neutron absorption cross section
Σ_1	Macroscopic neutron removal cross section for the high energy group
Σ_2	Macroscopic neutron removal cross section for the low energy group
τ	Neutron age
ϕ	Neutron flux
ω	Oscillator frequency, radians per second